U.S.N.A. --- Trident Scholar project report; no. 299 (2002)

Active Control of Fan Noise in Ducts Using Magnetic Bearings

by

Midshipman Jonathan P. Nelson, Class of 2002
United States Naval Academy
Annapolis, Maryland

Certification of Advisers Approval

Associate Professor John M. Watkins
Weapons and Systems Engineering Department

Associate Professor George E. Piper
Weapons and Systems Engineering Department

Acceptance for the Trident Scholar Committee

Professor Joyce E. Shade
Deputy Director of Research & Scholarship

USNA-1521-2

REPORT DOCUMENTATION PAGE

Form Approved OMB No. 0704-0188

1. REPORT DATE (DD-MM-YYYY)	2. REPORT TYPE	3. DATES COVERED (FROM - TO)
06-05-2002		xx-xx-2002 to xx-xx-2002

4. TITLE AND SUBTITLE
Active control of Fan Noise in ducts Using Magnetic Bearings
Unclassified

5a. CONTRACT NUMBER
5b. GRANT NUMBER
5c. PROGRAM ELEMENT NUMBER

6. AUTHOR(S)
Nelson, Jonathan P. ;

5d. PROJECT NUMBER
5e. TASK NUMBER
5f. WORK UNIT NUMBER

7. PERFORMING ORGANIZATION NAME AND ADDRESS
U.S. Naval Academy
Annapolis, MD21402

8. PERFORMING ORGANIZATION REPORT NUMBER

9. SPONSORING/MONITORING AGENCY NAME AND ADDRESS
,

10. SPONSOR/MONITOR'S ACRONYM(S)
11. SPONSOR/MONITOR'S REPORT NUMBER(S)

12. DISTRIBUTION/AVAILABILITY STATEMENT
APUBLIC RELEASE
,

13. SUPPLEMENTARY NOTES

14. ABSTRACT
See report.

15. SUBJECT TERMS

16. SECURITY CLASSIFICATION OF:			17. LIMITATION OF ABSTRACT	18. NUMBER OF PAGES	19. NAME OF RESPONSIBLE PERSON
a. REPORT	b. ABSTRACT	c. THIS PAGE	Public Release	70	email from USNA, Annapolis, MD, (blank) lfenster@dtic.mil
Unclassified	Unclassified	Unclassified			19b. TELEPHONE NUMBER International Area Code Area Code Telephone Number 703767-9007 DSN 427-9007

REPORT DOCUMENTATION PAGE

Form Approved
OMB No. 074-0188

1. AGENCY USE ONLY (Leave blank)	2. REPORT DATE	3. REPORT TYPE AND DATE COVERED
	6 May 2002	

4. TITLE AND SUBTITLE
Active control of fan noise in ducts using magnetic bearings

5. FUNDING NUMBERS

6. AUTHOR(S)
Nelson, Jonathan P. (Jonathan Philip), 1980-

7. PERFORMING ORGANIZATION NAME(S) AND ADDRESS(ES)		8. PERFORMING ORGANIZATION REPORT NUMBER

9. SPONSORING/MONITORING AGENCY NAME(S) AND ADDRESS(ES)		10. SPONSORING/MONITORING AGENCY REPORT NUMBER
US Naval Academy Annapolis, MD 21402		Trident Scholar project report no. 299 (2002)

11. SUPPLEMENTARY NOTES

12a. DISTRIBUTION/AVAILABILITY STATEMENT	12b. DISTRIBUTION CODE
This document has been approved for public release; its distribution is UNLIMITED.	

13. ABSTRACT: The objective of this project was to investigate global noise attenuation of narrow band fan noise in an air duct through the use of magnetic bearings. An axial flow fan creates tonal noise related to its rotational rate. Additional noise exists due to harmonics of this frequency as well as turbulent airflow. In addition to conventional brush bearings to support the fan shaft radially, this project used an active magnetic thrust bearing to control axial movement. The thrust bearing primarily functioned as an active sound control actuator. Active sound control is the method of achieving destructive interference of sound waves by outputting a secondary wave of equal amplitude and frequency, but 180 degrees out of phase with the primary wave. An error microphone was positioned in the duct to provide feedback to a Digital Signal Processor (DSP), which contained the active sound control program, while a performance microphone tested for global sound control at various points along the duct. Instead of using a secondary speaker, this project used the fan itself to collate the primary and secondary sound sources. Therefore, global sound control throughout the duct was theoretically possible. This project demonstrated this global control of noise experimentally.

14. SUBJECT TERMS	15. NUMBER OF PAGES
Active Magnetic Bearings, Active Sound Control, Least Mean Squares adaptive filtering	70
	16. PRICE CODE

17. SECURITY CLASSIFICATION OF REPORT	18. SECURITY CLASSIFICATION OF THIS PAGE	19. SECURITY CLASSIFICATION OF ABSTRACT	20. LIMITATION OF ABSTRACT

ABSTRACT

The objective of this project was to investigate global noise attenuation of narrow band fan noise in an air duct through the use of magnetic bearings.

An axial flow fan creates tonal noise related to its rotational rate. Additional noise exists due to harmonics of this frequency as well as turbulent airflow.

In addition to conventional brush bearings to support the fan shaft radially, this project used an active magnetic thrust bearing to control axial movement. The thrust bearing primarily functioned as an active sound control actuator.

Active sound control is the method of achieving destructive interference of sound waves by outputting a secondary wave of equal amplitude and frequency, but 180 degrees out of phase with the primary wave. An error microphone was positioned in the duct to provide feedback to a Digital Signal Processor (DSP), which contained the active sound control program, while a performance microphone tested for global sound control at various points along the duct.

Instead of using a secondary speaker, this project used the fan itself to collate the primary and secondary sound sources. Therefore, global sound control throughout the duct was theoretically possible. This project demonstrated this global control of noise experimentally.

KEY WORDS

Active Magnetic Bearings, Active Sound Control, Least Mean Squares adaptive filtering

TABLE OF CONTENTS

TABLE OF FIGURES

OBJECTIVE

The primary objective of this project was to investigate how active magnetic bearings could be used to globally reduce fan related noise created in an air duct. This project supported theoretical work regarding noise reduction along an air duct by demonstrating the attenuation of the fundamental noise frequency created by the fan.

PROBLEM

Duct systems are used in many situations to provide airflow to a particular space. However, fan and duct systems usually emanate unwanted noise. For example, auditoriums, in general, which are often noisy, must be quiet for an audience to hear a concert or a speaker. In addition, Naval ships need to quiet their ducts in order to provide more stealth and to reduce their inherent sound signature.

Heating, Ventilation, and Air-Conditioning (HVAC) systems typically have fans that will move air from the heating or cooling system to any desired space. Fan noise is characterized first by tonal noise, which is related to the fan's rotational speed. Anyone who has stood near a fan has noticed this fact that as the speed of the fan is increased, the frequency of sound created increases. That is, the whine of the fan blades sounds higher in pitch as the fan turns at a higher rate.

In addition to the fundamental frequency, there exists a blade rate, which is the fundamental frequency multiplied by the number of fan blades. The fan also creates harmonics that are exact multiples of the blade rate. Turbulent airflow in the duct produces noise over a broad range of frequencies. The duct acts like a filter, amplifying and/or attenuating the magnitude of the noise

at different frequencies. Thus, besides the fundamental frequency, the fan creates a broadband spectrum of unwanted noise.

BACKGROUND

This project explored the attenuation of fan-related noise through the use of a magnetic thrust bearing, which had the capability of controlling the fan impeller's position. By using the magnetic bearing to vibrate the fan shaft at a certain frequency, this vibrational noise could cancel out the primary noise of the rotating fan.

ACTIVE SOUND CONTROL

For sound control applications, the primary noise is the noise that is to be attenuated. In this

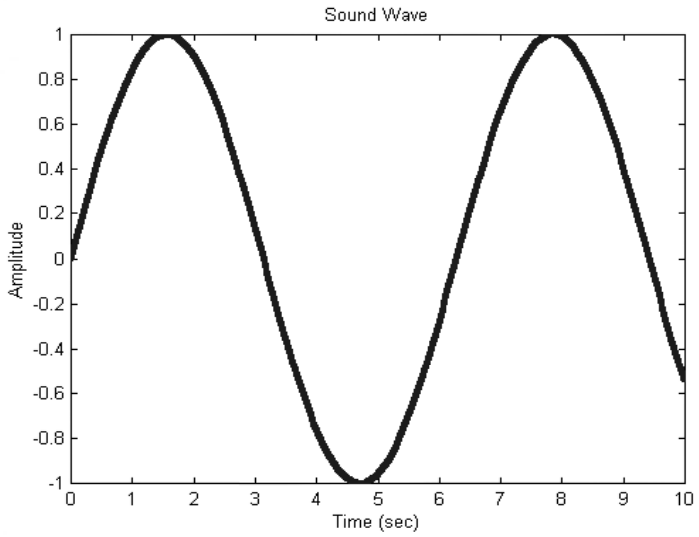

Figure 1

project, the primary noise was the fan noise related to the fan's rotational speed. Although it seems paradoxical, active sound control is achieved when the primary noise is cancelled out by another noise, known as the secondary noise. In other words, sound can be lowered if more noise

is present. The exact characteristics of this additional noise will be discussed later.

Sound, in general, is nothing more than pressure waves traveling through a given medium, such as air or water. Typically, sound waves are sinusoidal in nature, as Figure 1 demonstrates. For example, waves in the ocean behave similarly to sound waves in that they both have troughs and peaks, an amplitude, and a frequency of oscillation. [3] A duck sitting on the water will experience up and down motion as the wave passes through it, but will itself experience no net displacement. This is the same principle with sound waves in a duct. When a sound wave originates in a duct, it disturbs the air particles immediately around it, which in turn transfer energy to the particles adjacent to them and so on. This process (which takes place at the speed of sound) is responsible for the propagation of sound.

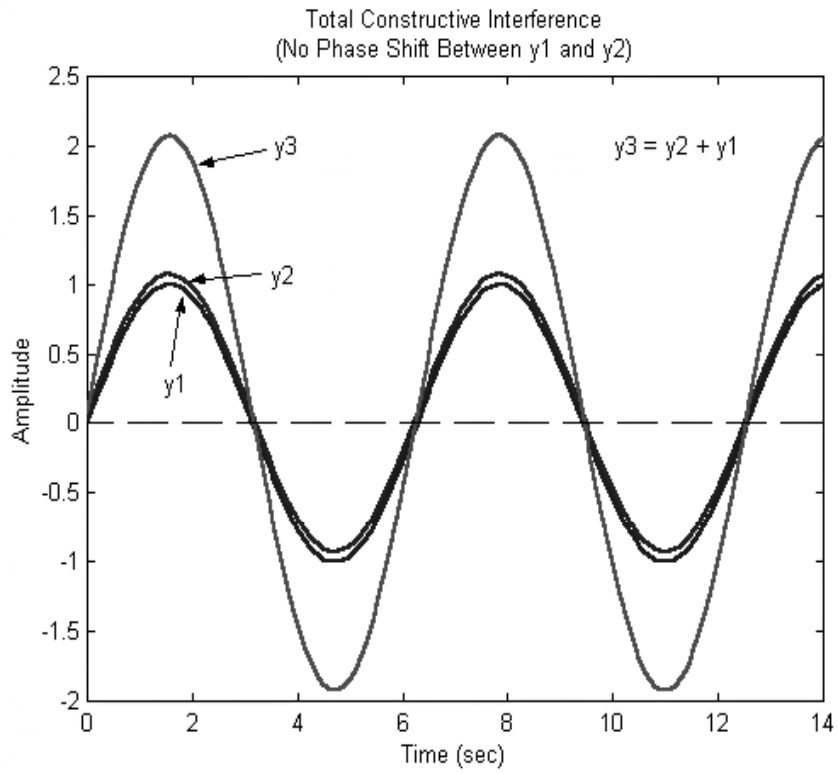

Figure 2

Because a sound wave has troughs and peaks, one can use the principle of interference to amplify or quiet sound. When two waves cross paths, their amplitudes add to produce a resulting amplitude. If they cross so that the peak of one wave lines up with the peak of the other wave, then constructive interference occurs. The two waves are said to be “in phase”, having a net phase difference of zero degrees. That is, the resulting amplitude is equal to the amplitude of the first wave plus the amplitude of the second wave. Figure 2, therefore, demonstrates the principle of total constructive interference since the phase difference between the two original waves is zero.

When these two waves meet so that the original peaks do not line up exactly, then the resulting amplitude is not quite as high as the sum of the individual amplitudes although it is still higher than either one of the original two amplitudes. Note that at this point, constructive interference still occurs. Here, the phase difference is between zero and 120^{o} or between 240^{o}

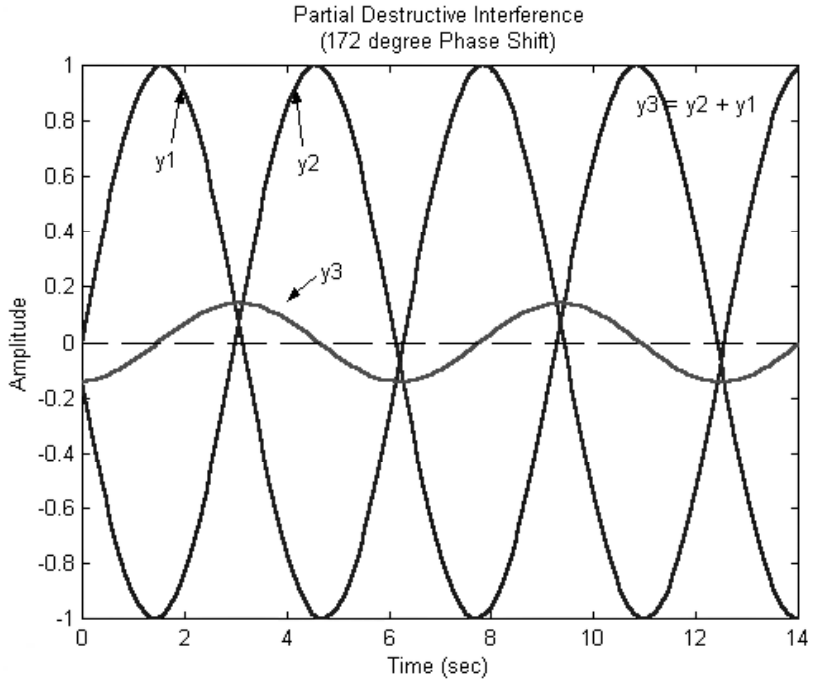

Figure 3

and 360^{o}. There comes a point, however, when the resulting amplitude begins to get smaller than either of the two original amplitudes. At this point, destructive interference occurs and the resulting phase angle difference between the two waves is between 120^{o} and 240^{o}. When the two waves are exactly 180^{o} out of phase, the trough of one wave meets with the peak of another wave and they cancel each other out (assuming equal amplitude and frequency.) At this point, no sound is heard from either wave. [3] Figure 3 demonstrates the concept of adding a wave with another that is 172^{o} out of phase. Note that the resulting amplitude (y3) is much smaller than either of the two original waves. Only when the phase shift is 180^{o} will the resulting amplitude be zero. Therefore, in order to attenuate a sound wave, a secondary wave must be propagated that is equal in amplitude and frequency to the primary wave but 180^{o} out of phase in order to ensure total destructive interference and thus, sound cancellation.

Returning to an earlier point, it should now make sense that by adding additional noise to a system, the total noise can be attenuated, as long as the two sound waves interfere destructively. Concerning the energy of the system, it appears that the law of energy conservation has not been followed since both the primary and secondary noise had a certain original amount of energy associated with them. Since the total noise is quieter than either of the two, there seems to be less energy in the system. However, although the resulting energy does not go into making noise, it still exists in a potential form. In addition, each original sound wave still exists and so the energy associated with each one also exists, even after they destructively interfere. However, the energy of the sound wave is not converted into sound. Therefore, the law of energy conservation still applies to sound control applications.

The placement of the secondary sound source plays an important role in noise cancellation as the diagram below demonstrates. If the distance between the primary and secondary sources is

much smaller than the wavelength of the sound emitted and the two sources are 180^{o} out of phase, then the two waves will almost overlap at all points in space, thus achieving global noise control. Note that in Figure 4, the red and blue circles overlap at multiple locations perpendicular to the line of noise sources.

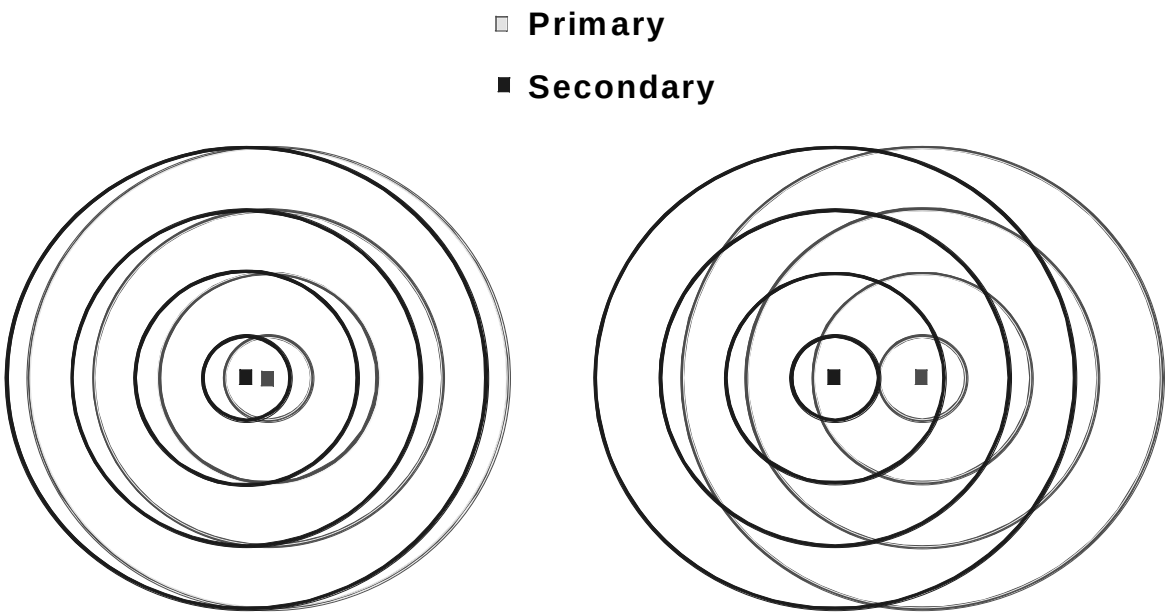

Figure 4 – Collocation of Sound Sources

In addition, the left and right regions of the noise sources show that destructive interference will still occur since the waves almost overlap. Therefore, the source separation is small compared to the wavelength of sound.

However, if the noise sources are spaced apart at a distance greater than the wavelength, then destructive interference will only occur at a few discrete points as the diagram above and to the right shows. In addition, constructive interference will also take place at other points, which is quite contrary to the purpose of a secondary sound source.

ACTIVE MAGNETIC BEARINGS

As opposed to conventional ball bearings, active magnetic bearings use the forces of electromagnetic attraction to suspend a rotating shaft between the surrounding electromagnets. Typically to support a rotating fan, a magnetic bearing system uses two radial bearings which surround the shaft to stabilize it in the x and y direction. Because the fan pushes air in one direction, Newton's third law states that an equal force will push the fan itself in the opposite direction. Therefore, the active magnetic bearing system must use, as well, a thrust bearing that allows for control of the shaft in the z direction. [4] Figure 5 shows how a typical active magnetic bearing system supporting a rotating shaft can be used for active noise control. The microphone senses the noise and sends a signal to the noise controller, which controls the active magnetic bearings in order to attenuate the noise at the microphone.

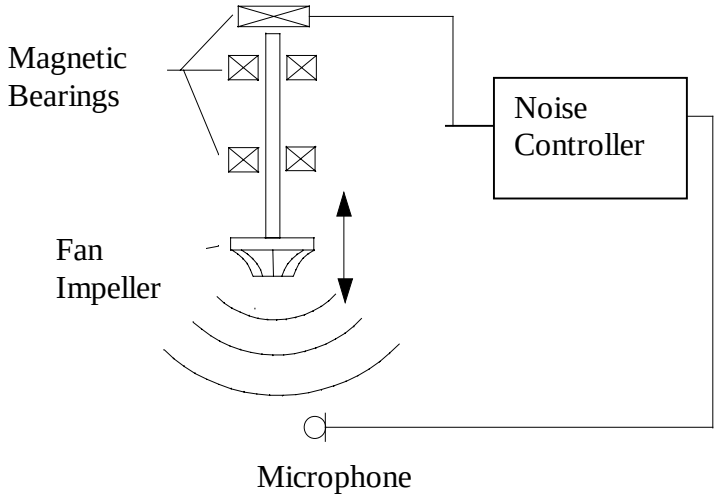

Figure 5 – Active Magnetic Bearing System

There are many advantages of magnetic bearings. Because there is no contact between rotating parts, the life of the machine is increased. In addition, there is no need for a complex lubrication system such as those found in automobile engines. When using conventional ball

bearings, there are critical speeds at which the shaft experiences large vibrations. Magnetic bearings can be used to reduce these vibrations or change the critical speeds. In addition, they allow the system to rotate at a much higher rate than their conventional counterparts. [2] Another benefit of using active magnetic bearings is that the position of the shaft can be controlled in the x, y, and z directions. That is, because they can damp out unwanted vibrations, they are just as capable of producing desired vibrations. This is beneficial because the controlled bearings can be vibrated in such a way to deaden noise in the pipe by creating anti-noise. That is, the noise from the secondary noise source (the magnetic bearings) is of the same frequency and amplitude as any given primary noise source. However, it must be 180^{o} out of phase with the primary source, to produce complete destructive interference. From physics, it is known that when two waves cross paths with this type phase difference, the resulting amplitude is zero. Therefore, noise is damped out.

The active magnetic bearing system is highly nonlinear due to the quadratic relationship between electromagnetic force, current and position:

$$f = k*i^2/x^2 \qquad (1)$$

where x is the distance between the bearing and rotor, i is the current through the bearing's coils, and k is a constant. It is difficult to analyze unless the nonlinear system can be approximated by a linear system operating about a certain point. [1]

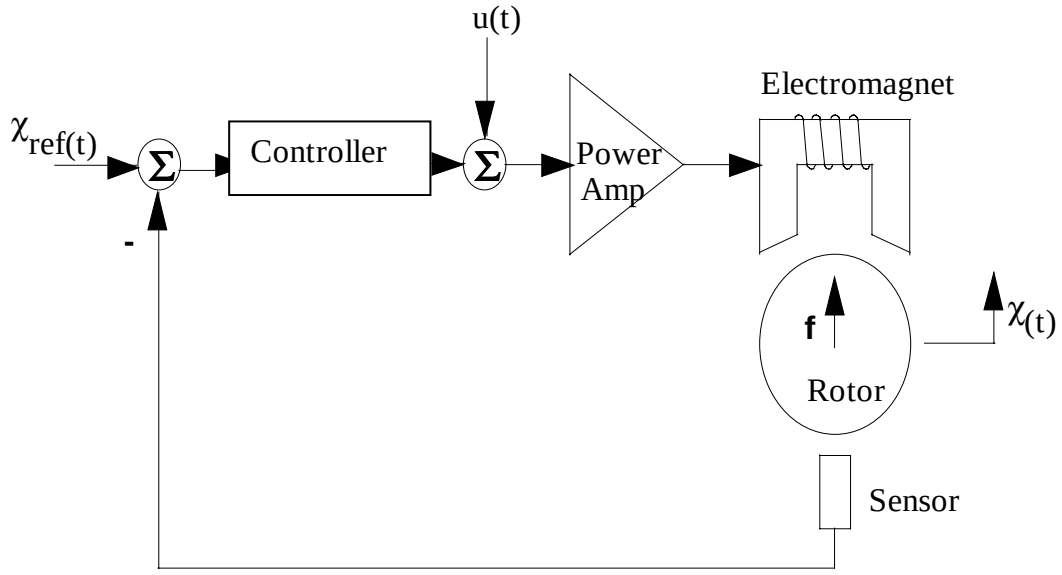

Figure 6 – Magnetic Levitation System

In addition, the active magnetic bearing system is inherently unstable and therefore requires feedback control to operate as Figure 6 demonstrates. According to the diagram, the position of the rotor is fed back to the controller through a sensor. The controller then inputs a difference between the desired position, Xref(t), and the actual position, X(t) into an equation, which outputs a voltage. This voltage is added to a bias voltage, u(t), which governs how much voltage exists when the rotor's position is at equilibrium. Because the controller electronics cannot supply nearly enough current for the electromagnet to operate properly, a power amplifier is needed to supply the current that the electromagnet needs. Finally, note that this diagram has only one electromagnet controlling the position of the rotor.

Although the logic is the same for a magnetic thrust bearing, the following discussion will be concerned with a radial magnetic bearing in which electromagnets entirely surround the rotor without feedback. If the rotor shifts in any x or y direction from its centered position within the bearing, the side that it is closest to will attract the shaft more than the side opposite it since the

distance is smaller. As the magnet on this side pulls the shaft closer toward it, the distance between the shaft and this magnet gets even smaller, causing the magnet opposite this side to have even less of an effect. Eventually, the shaft is physically touching this magnet, creating huge amounts of friction, which can cause damage to the shaft and the bearing system.

The stability of an active magnetic bearing system is analogous to keeping a ball steady on the top of a hill. As any disturbance in nature pushes it one way or the other, the ball rolls down the hill, never to return to its original equilibrium position without energy from an outside source. To correct for instability requires the use of a feedback controller so that the system is stable over the entire operating region, which is a small physical region around the equilibrium point.

In this project, the fan's impeller is in the equilibrium position when the circular magnet is perfectly centered within the thrust bearing. Note that the controller only works for the operating region, where the system has been linearized. Outside that region, instability still exists.

MIDN WIGGINS' TRIDENT PROJECT

This project built on a Trident Scholar project completed by Midn Wiggins in the spring of 1998. [6] Wiggins demonstrated the ability to quiet noise from a fan in an open field. In other words, his fan operated in open space, with no enclosures (such as an air duct) surrounding it. Through the use of magnetic bearings, he quieted a fundamental frequency at the source of its origination (the fan itself), and he demonstrated this novel noise reduction technique at one particular point in space. However, his project did not explore the aspects of global noise attenuation, as this project did. That is, he did not demonstrate the ability to reduce the noise at different points in space, but rather at one select point.

In addition, he controlled the magnetic bearings using analog circuitry, whereas this project used digital means through the use of a real-time digital signal processor.

SYSTEMS DESIGN – OVERVIEW

Figure 7 shows a schematic of the acoustic duct with the motor, fan impeller, and magnetic bearings located inside the duct. The active magnetic bearing system, not shown, was the control mechanism used to stabilize the thrust bearing, indicated in Figure 7 by the letter 'T'. The thrust bearing's closed loop consisted of feedback sensors, which input the position of the impeller within the bearing to a digital signal processor (DSP). Specifically, the position was input into a digital compensator responsible for stabilizing the thrust bearing. Bias voltages for each side of the thrust bearing were added to the output of the compensator in order to boost the voltage sent to the bearing. Finally, this signal exited the processor and was sent to power amplifiers, where the current was amplified to values that the bearing needed to operate properly.

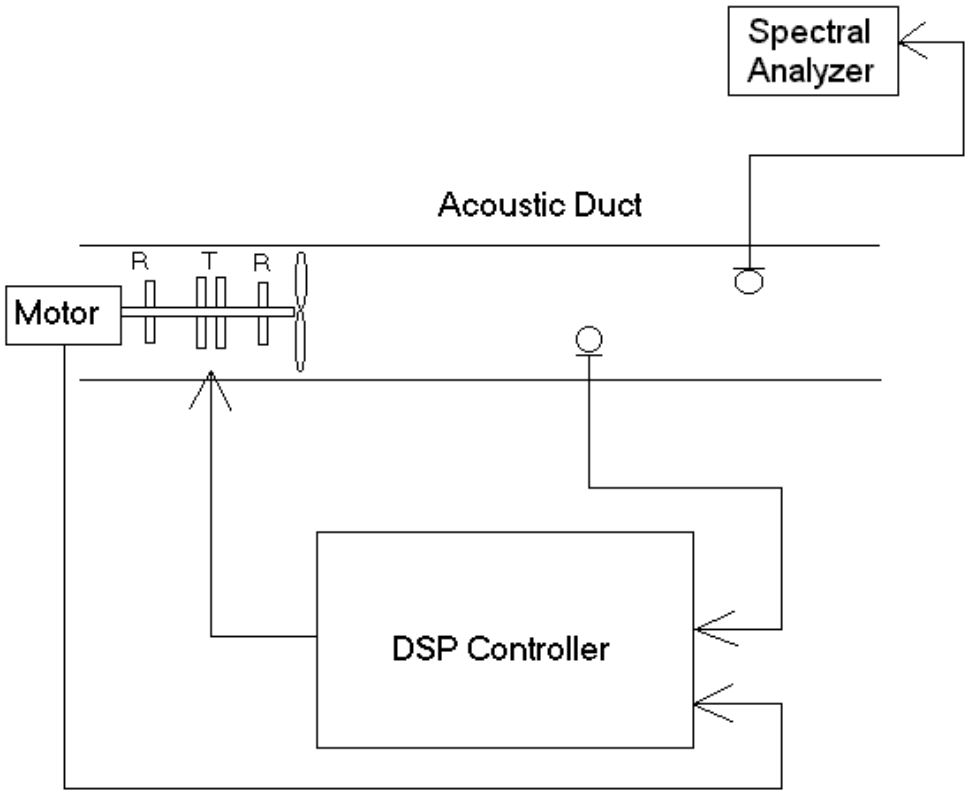

Figure 7 – Duct, Controller, and Microphones

The active sound control system, shown in Figure 7, consisted simply of a DSP controller (different from the one that stabilized the thrust bearing) and two microphones. The inputs to the controller were (1) a sine wave, representing the frequency of the fan speed, and (2) the error microphone, which was feedback for the sound control algorithm.

System Design – Active Magnetic Bearings

Overview

Active magnetic thrust bearings were used to control the axial movement of a fan shaft, which was connected on one end to a motor and on another end to a fan blade. The fan blade was positioned so that it rotated within a PVC air duct. Sensors, which monitored the position of the rotor within the thrust bearing, sent a signal to a Digital Signal Processor (DSP) controller that stabilized the position of the rotor so that it remained in the center of the bearing at equilibrium. Finally, power amplifiers were needed to supply the large amount of current that the thrust bearings needed to generate appreciable force.

Motor and Fan

A DC motor was used to turn the fan shaft and fan. The fan shaft was supported by two radial journal bearings, which were simply a “sleeve” for the shaft to fit snugly through. Because a journal bearing is made of a rather soft metal, such as brass, whereas the iron shaft is quite hard, the coefficient of friction between the two metals was quite low and the shaft could rotate without too much resistance.

An active magnetic thrust bearing was attached to the fan shaft in between the two radial journal bearings. Although its function will be described at a later point in greater detail, the thrust bearing consisted of a rotor (attached to the fan shaft) that was located in between two electromagnets, which were used to control axial movement of the fan shaft. In this project, the thrust bearing first stabilized the rotor so that it is centered in between the thrust bearing when at equilibrium. Then, the thrust bearing will be used to vibrate the fan shaft in such a way that it

produces a tone that is completely out of phase with the inherent fan noise. The result will be sound attenuation.

THRUST BEARINGS

As previously mentioned, an active magnetic thrust bearing is used to control the fan's axial movement. Using two electromagnets, the thrust bearing is able to pull a disk, or rotor (attached to the fan shaft) in either axial direction. The purpose is not only to stabilize natural vibrations, but also to control them actively for active sound control. Each electromagnet is roughly two and a half inches in diameter. (See Figure 8.) Each magnet has a center hole of radius $r_1 = 0.4062$ inches, in which the fan shaft rotates. Surrounding this hole is a metal ring of radius $r_2 = 0.75$ inches (A_1) and another ring of radius $r_4 = 1.23$ inches (A_2), both of which provide the medium for the flow of magnetic flux from the magnet to the rotor.

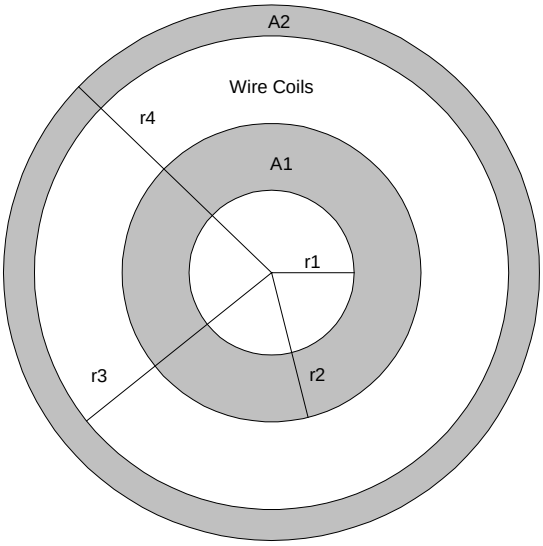

Thrust Bearing
Cross Sectional View

Figure 8

In between the two metal rings are the turns of wire. The bearings used for this project contained N = 70 turns of wire in each bearing. The cross-sectional area of the magnets was determined according to equations (2) and (3):

$$A_1 = \pi*(r_2^2 - r_1^2) = 1.248 \text{ in}^2 \quad (2)$$

$$A_2 = \pi*(r_4^2 - r_3^2) = 1.240 \text{ in}^2 \quad (3)$$

Since the difference between the two areas is 0.645%, they are assumed to be equal.

The resistances of each side of the thrust bearing were measured with a standard ohmmeter. The resistance of thrust bearing one was 3.13 Ω, while the resistance of thrust bearing two was 3.83 Ω.

When current flows through an electromagnet in the presence of a metal object (such as the rotor attached to the fan shaft) magnetic flux lines travel out of one side of the electromagnet, through the metal object, and then return to the other side of the electromagnet, all in a closed loop. For this application, flux flows out of A_1, travels through the rotor, and returns through A_2. However, there exists, in addition to this magnetic flux, what is known as leakage flux. That is, some of the flux will travel out of the electromagnet and then return again in a closed loop without ever traveling through the rotor. The total inductance, therefore, is composed of the magnetic flux (flux through the rotor) and the leakage flux, which does not travel through the rotor at all. In order to measure the overall inductance for each side of the thrust bearing, a standard LRC meter was used to measure certain inductances under different conditions. Note that under all the following conditions, both thrust bearings were present and spaced at their nominal distance, which was $2x_0$, or 0.056 in. Figure 9 shows the side view of the thrust bearing and the rotor and was the model for the following conditions:

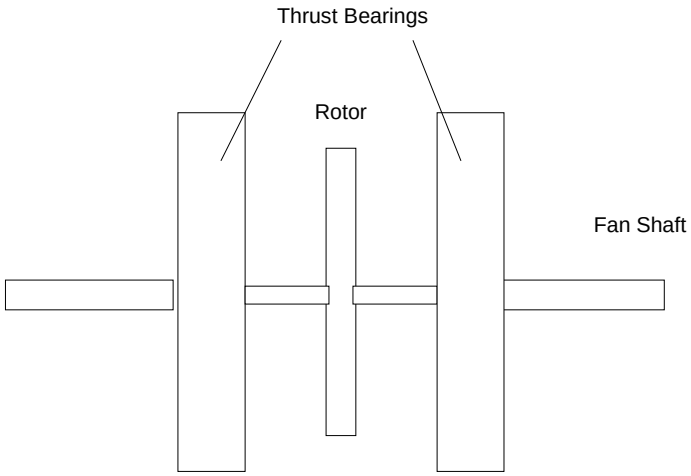

Thrust Bearings
Side View

Figure 9

Condition #1: Rotor is absent

Condition #2: x = 0 → Rotor is touching bearing whose inductance is being measured

Condition #3: $x = x_0 = 0.028$ in → Rotor is spaced equidistant from both bearings

Condition #4: $x = 2x_0 = 0.058$ in → Rotor is spaced farthest away from bearing whose inductance is being measured (touching other electromagnet)

Condition Number	Average Inductance (μH) Thrust Bearing One	Average Inductance (μH) Thrust Bearing Two
1	611.67	584.67
2	707.33	645.67
3	687.33	635.00
4	670.67	622.33

From these inductances, it possible to apply the equation to solve for k and k_0: [7]

$$L(x) = L_l + L_m(x) \quad (4)$$

where $$L_m(x) = k/(k_0 + x) \quad (5)$$

Therefore,

$$L(x) = L_l + k/(k_0 + x) \quad (6)$$

The k and k_0 constants are summarized in the following table:

	k	**k_0**
Thrust Bearing One	2.66E-7 (m*H)	0.002785 m
Thrust Bearing Two	2.119E-7 (m*H)	0.00347 m

Instead of solving equation (6) with two equations and two unknowns, the values for k and k0 could be directly calculated by noting the following equations: [7]

$$k = 0.5*N^2\mu_0 A_i \quad (7)$$

where

N = number of turns of wire
μ_0 = permeability of free space, 4πE-7 Wb/A*m
A_i = cross sectional area of electromagnet

and

$$k_0 = l_i / (2* \mu_r) \quad (8)$$

where

l_i = mean length of the magnetic material
μ_r = relative permeability of magnetic material

However, it is difficult to calculate k and k_0 directly using equations (7) and (8) because the individual terms of the equation are difficult to measure. For example, the number of turns of wire is assumed to be N = 70 according to original design specifications. However, the only way to verify that number is to take the bearing apart and count the turns. It was not advantageous to do this since the bearings are sensitive to slight variations in physical properties. In addition, μ_r, the relative permeability of magnetic material ranges from 500 to 4000 for iron or steel. With such a broad range, it was virtually impossible to estimate this value and use it to calculate an accurate value for k_0. Therefore, solving the L(x) equation with two equations and two unknowns was the best method for finding k and k_0. A MATLAB script file was written, shown in Appendix 2, to describe these and other pertinent parameters needed for simulations and design.

SENSORS

In the project, Bentley-Nevada eddy current sensors were used to measure the position of the rotor within the thrust bearing. As the rotor moved, the output voltage of the sensor changed, allowing the controller to determine where it was and what magnetic forces were needed to restore its position back to equilibrium. To calibrate the sensors, it was noted that the sensor output was 0V when the metal object was touching the sensor, and –14V when the distance from the sensor to the object was 1/16" or greater. Since the sensors were inserted into thrust bearing one, the distances used throughout this project were referenced from this end. That is, x=0 means that the rotor is touching thrust bearing one.

The output voltage from the sensors was to be read by the DSP controller through a Digital to Analog (D/A) converter. The range of voltages that this converter could read was -10V to +10V. Therefore, the output voltage range from the sensors had to be scaled down and shifted to fit this new range. In order to prevent accidental saturation, however, it was determined that a one volt buffer would be used on either side of the range, making the new range –9V to +9V. That is, when the rotor was closest to the sensor, the output range was adjusted to be –9V. When the rotor was centered between the two bearings, however, the output voltage was ideally 0V. Finally, when the rotor was touching the bearing opposite the sensor, the output voltage was adjusted to be +9V.

Because thickness of the rotor was not exactly uniform and because the rotor's position was not always perfectly vertical in between the thrust bearings, two sensors were used. One measured the distance at the top of the rotor while the other measured the distance at the bottom. The output of these two sensors were voltages, which were used the average distance of the rotor's position within the bearings. In order to shift the sensor output voltages to –9V to +9V, a

scale and shift circuit was built using Op-Amps and is shown below in Figure 10. V_1 represents the output voltage from the first sensor and similarly, V_2 is the output voltage from the second sensor. V_{out} is the output voltage of the circuit to be read by the DSP controller.

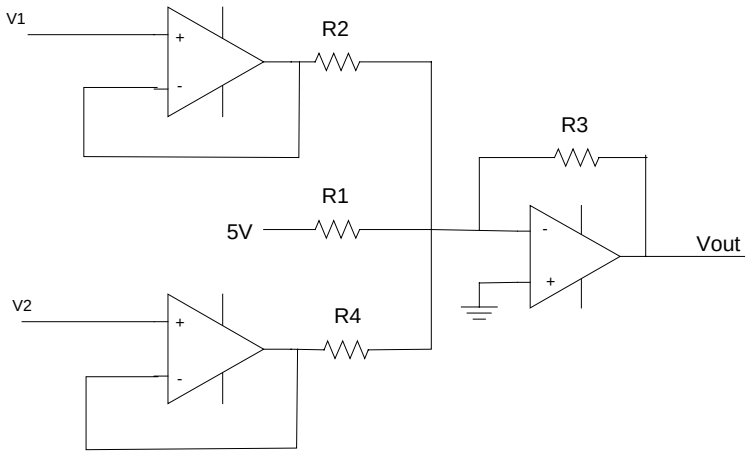

Scale and Shift Circuit

Figure 10

DIGITAL SIGNAL PROCESSOR

The output of the scale and shift circuit was to be read by a digital signal processor (DSP) board and used to implement a digital controller. This board was manufactured by dSPACE Inc. More specifically, the digital controller was a computer program developed in MATLAB's Simulink toolbox and then downloaded to the DSP controller board. Its main function was to stabilize the magnetic bearings by shifting the system plant's root locus[1] to the Left Half side of the complex plane[2] so that the operating point exists in a stable region. Because it operated digitally, the DSP first used an Analog to Digital (A/D) converter to convert the analog output from the scale and shift circuit into a digital. The computer used this digital number into a

[1] The root locus shows all the roots and zeros of any system given any gain, k. It demonstrates areas of stability.

computer program and returned a digital output. Finally after some processing, this output was converted back to an analog number via a Digital to Analog (D/A) converter. An analysis on the type of controller used is provided in one of the following sections.

The overall design is shown in Appendix 9. Note that the figure also shows that the output voltage of the controller (Δe) was added to the bias voltage of the first bearing, while it was subtracted from the second bearing. By this method, known as differential driving, as the rotor moved out of its equilibrium position toward one of the two bearings, that bearing received less voltage and therefore pulled less while the other one received more voltage and therefore pulled more. The bias voltages were determined experimentally by letting the bias voltage for thrust bearing one be 1V. At equilibrium, the electrical equation, (9), reduced to e = R*i. By knowing the resistance of the first thrust bearing, it was possible to find the corresponding current. Knowing this current, the current through the second thrust bearing was found by setting the force equations for each bearing equal to each other (Equation 11.) Appendix 3 shows the computer program that used the currents through each bearing to determine the magnetic force produced by each of the bearings. Appendix 4 calculated the force in each bearing given its current. Both of these programs were used to help experimentally determine the bias voltages at equilibrium. Note that the equilibrium currents were not the same value since the inductances, and therefore the k and k_0 values, were different for the two bearings. From this current, it was then possible to use Ohm's law again, to find the corresponding bias voltage across the second thrust bearing: 1.6371 V. Although these values served as a basis for the theoretical design, in practice, they had to be adjusted. Values of 1V for each bias voltage allowed the system to

[2] The complex plane is made up of purely real numbers on the x-axis and purely imaginary numbers on the y-axis. Complex numbers are points made up of both real and imaginary components.

operate properly. The remaining components of Appendix 9 will be discussed in the following sections.

After the bias-voltage summing junction, the voltage output was sent to the D/A converter. From there, the signal went to a power amplifier.

Power Amplifiers

The amount of current needed to operate the magnetic bearings ranged from around one amp when the rotor was at equilibrium to two or three amps when the rotor was not at equilibrium. Because the output of the DSP controller board could not supply enough current to the bearings, power amplifiers were needed. The original design called for two APEX SA50 Pulse Width Modulated power amplifiers, capable of supplying up to 5A of current. The output of the amplifiers went directly to the thrust bearings. A pulse width modulated signal operates by toggling a switch very rapidly. When the switch is on all the time (100% duty cycle), the output voltage is the maximum amount and conversely, when the switch is off all the time (0% duty cycle), the output voltage is zero. Any duty cycle in between means that the voltage is turned on a certain percentage of the total period. For example, a 30% duty cycle means that the voltage is turned on for 30% of the period and off for 70%. Therefore, if the maximum voltage supplied is 5V, then a 30% duty cycle will supply (0.3)(5V), or 1.5V. In general, pulse width modulated signals are very efficient and can supply a relatively large amount of current for high power applications. However, in extensive testing, the SA50 power amplifier did not work well for loads with high inductance and small resistance. When a simple motor, whose resistance was 90Ω, was connected to the power amplifier, the pulse width modulated signal was correct in varying from 0 to 5V for any given duty cycle. However, when connected to the thrust bearings,

whose resistance was only around 3Ω, the power amplifier experienced adverse loading effects in that the 5V range shifted down to about –2V to 3V. Therefore, while the 5V range was still maintained, part of it had become negative.

To fix this problem, it was suggested that a power resistor be added to increase the overall resistance of the bearings. While this would no doubt fix the loading effects problem, it would unfortunately cause the current to decrease by a large amount in accordance with Ohm's law. Therefore, to compensate, the voltage signals coming out of the controller would have had to be increased, even to the point of saturation.

In addition, another problem with these power amplifiers was that they proved to be too noisy for sound control applications. Because they turn on and off very rapidly to produce an average voltage between 0 and 5V, they also produce a lot of undesirable noise.

To fix these two problems, the SA50 power amplifiers were replaced with APEX PA26 power amplifiers. These linear amplifiers had no pulse width modulated signal, which meant that they operated silently. In addition, they experienced no loading effects and could therefore operate very well with the low-resistive thrust bearings. A disadvantage of the PA26 power amplifier was that it was quite inefficient. A great deal of its input power was lost due to heat, meaning that unless large heat sinks were used, the power amplifier would burn up. However, with these heat sinks and a fan blowing across them, the PA26 power amplifier operated quite well.

The power amplifiers received their input signal from the output of the dSPACE controller. The outputs of the power amplifiers were connected directly to the thrust bearings.

SYSTEM PLANT

The physical equations that describe the behavior of the thrust bearings are known as the system plant. The input to the plant was a change in voltage, while the output was a change in the rotor's position in between the two thrust bearings. Actual equations consisted of two types: electrical and mechanical.

The electrical equations were state equations, which are nothing more than first-order ordinary differential equations describing the change of certain state variables:

$$L(x)di/dt = e - Ri + kiv / (k_0 + x)^2 \qquad (9)$$

where,

i = current
R= resistance of coil
e = voltage
v = translational velocity of rotor
k, k_0 = constants (Thrust Bearing section, pg 21-22)
L(x) = total inductance of coil

In this case, the differential equation, (9), described the voltage drops through the electrical portion of the plant. For example, due to the resistance of the windings, there is a small voltage drop. In addition, there is a voltage due to the inductance of each thrust bearing. Finally, there exists a voltage drop due to the back EMF presented when the rotor changes position.

Mechanically, the rotor experienced four forces pulling on it. The first two were due to the force of the magnetic bearings, each opposite to each other. The third was the restoration force of the coupling device. Separating the motor and the fan shaft was a coupling device that acted almost like a spring. Its purpose was to allow the fan shaft to move axially, for without it, the rotor and shaft would be rigidly attached to the motor. The coupling device, therefore, had a force associated with it equal to some spring constant multiplied by the change in distance from

the spring's equilibrium position. To determine the spring constant, weights of varying amounts were placed on the spring and the deflection in spring's length was measured. Since two points define a straight line, two weights were used, one of 2.5 lbs and one of 5 lbs. Using the corresponding change in lengths that these forces produced, it was possible to fit the data to a line F=a*D + b, where F is the force, D is the distance, and a and b are constants. It was found that the spring constant was 80 lbs/in (13,858.24 N/m). This method proved to be quite crude and somewhat inaccurate as is demonstrated in the following paragraph.

The fourth and final force on the rotor was due to the damping of the coupling device. In order to find the damping coefficient, the output of one sensor was viewed on an oscilloscope. The rotor (attached to the spring) was pulled away from its equilibrium position and then released, allowing it to oscillate until reaching equilibrium again. The waveform produced during this experiment showed a decaying sine wave, the peaks of which would match an exponential decay. Therefore, it was possible to use Microsoft Excel to plot the peaks and then find a exponential best fit of the form: $y=a*e^{-st}$, where *a* and *s* are constants. (See Appendix 6.) With a few calculations, it was possible to find β, the damping coefficient. It is interesting to note that in finding the damping coefficient, it was easy to calculate the natural frequency of vibration, ω_n. This term can be used to find the spring constant, k, directly. Running this experiment multiple times resulted in a k ranging from around 20,000 N/m to almost 23,000 N/m. Since this method involved much more accurate means of finding the spring constant than stacking weights on the spring and measuring the change in position with a ruler, it was decided that these values of k would be used for modeling the system for the remainder of the project.

The mechanical equation was:

$$mdv/dt = -fm_1 + fm_2 - f_s - f_d \qquad (10)$$

where,

m = mass of the fan shaft, rotor, and fan blade
v = translational velocity of the mass
fm_1 = magnetic force of the first thrust bearing
fm_2 = magnetic force of the second thrust bearing
f_s = restoration spring force of the coupling device
f_d = damping force of the coupling device

and,

(11)

$f_m = 0.5k*i^2 / (k_0 + x)^2$ (12)

$f_s = ks*\Delta x$ (13)

$f_d = \beta*v$

Using the electrical and mechanical equations, (9) and (10) respectively, the plant was simulated using MATLAB's Simulink toolbox. (See Appendix 7.) However, because it is highly non-linear, it was necessary to linearize the system around an operating point. A Matlab m-file was written that would complete this task using the 'jacobian' command. (See Appendix 5.) The result, therefore, was a series of linearized state equations. However, it was possible to use MATLAB commands to convert these equations into a plant transfer function relating an input voltage to a change of the rotor's position.

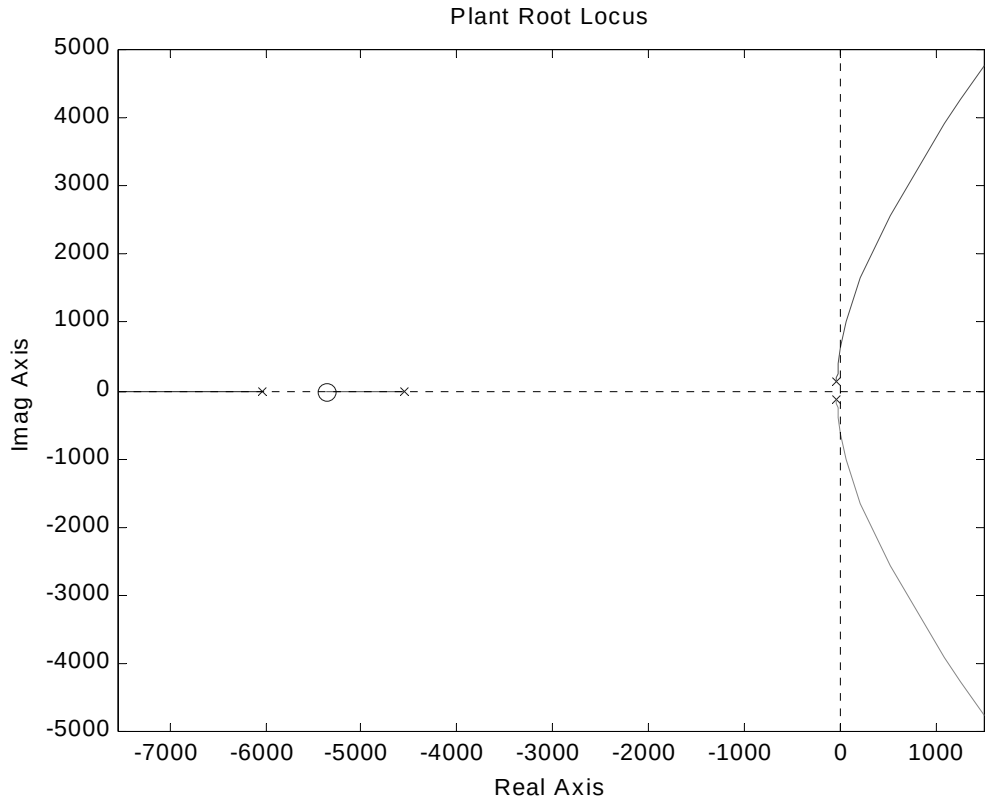

x = pole
o = zero

Figure 11 – Uncompensated System Root Locus

The root locus of Figure 11 shows the poles and zeros of the uncompensated plant. Note that the electrical poles are far into the left-half plane, while the mechanical poles are closer to the imaginary axis.

MAGNETIC BEARING CONTROL ALGORITHM

The type of digital controller that the design originally called for is known as a lead compensator. It was designed using design point methods of classical linear control theory. The first thing needed in order to find the controller was a design point, a complex point in the s-plane. The first criterion in choosing this point was that the damping ratio for the system as a

whole should be $\zeta = 0.7$ so that the maximum overshoot of the rotor when returning to its equilibrium position would be only 4.598%. Choosing a natural frequency, ω_n, equal to 600 rad/s, gave a design point of $s_d = -420 + j428.49$. A Matlab m-file was used to find what is known as a lead controller that corresponded to this design point. A lead controller is of the form:

$$k_c*(s+z) / (s+p)$$

where k_c, z, and p are constants.

Using this controller, the root locus of the system (plant and controller) was plotted and is shown below in Figure 12. As the figure demonstrates, the lead controller bends the plant root locus farther into the left-half plane where the poles and zeros must be located for stability.

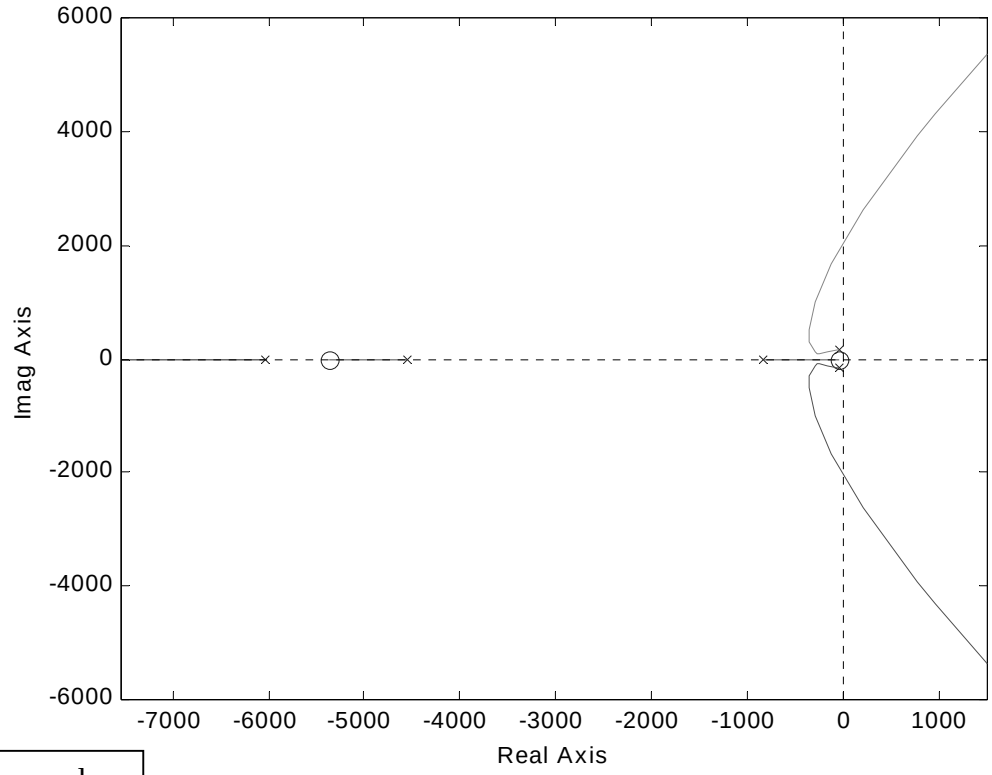

Figure 12 – Lead Compensated System Root Locus

The disadvantage of using this type of controller is that it does not account for steady state error. That is, this type of compensator will not keep the rotor in the center of the thrust bearing, but will steady out at some other position. For sound control, it was found that the rotor had to be exactly centered so that when a sine wave was inputted into the controller to oscillate the rotor, the rotor would not crash into either side of the bearing inadvertently. The reason is that any steady state error could lead to problems with the assumed and actual position of the magnet at any given time. In other words, when the sound control algorithm sent a sine wave into the controller, it assumed that the magnet was in the center of the bearing. This assumption was necessary in order to create a sine wave that was no bigger than the total air gap with the bearing. If the bearing was not perfectly centered, as it should be, then the sound control sine wave caused the magnet to crash into the sides of the bearings.

To correct for this steady state error, a PI (Proportional plus Integral) controller was used, which had the form:

$$k_p+k_i/s$$

Whereas a gain controller consisted of simply a multiplicative gain, k_p, the PI controller contained an extra term, k_i/s. In the Laplace domain, the 1/s term denotes an integral. As k_i increases, the steady state error will be eliminated faster, but the resulting system will be more unstable. The system's open-loop frequency response, shown in Figure 13, helped provide guidelines for determining the values of this controller. The value for k_p was set at 800 while k_i was set at 1000. The proportional part consisted of simply a gain, k_p, that would move the operating point along the root locus until it remained stable, while the integral portion, k_i/s, was

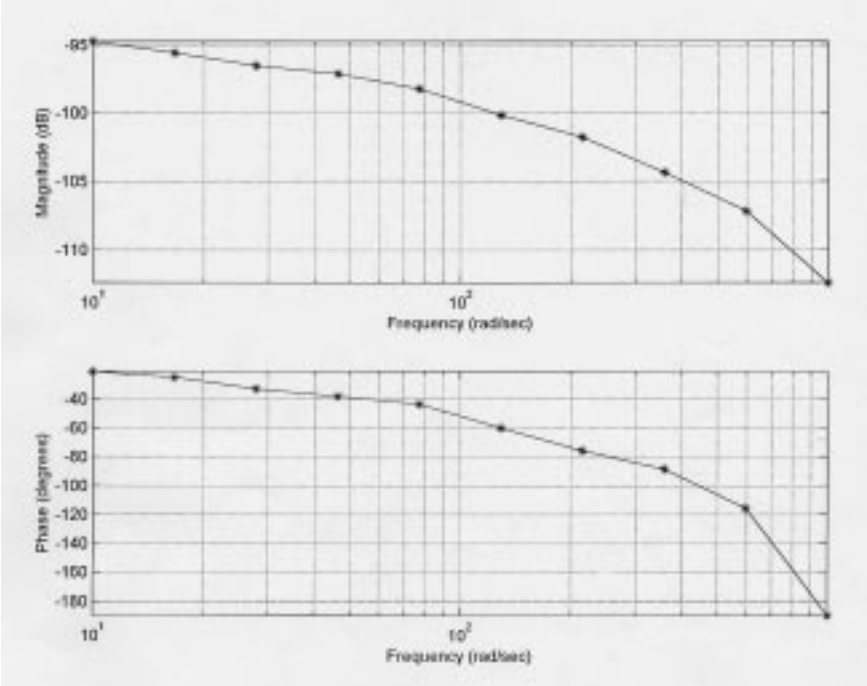

Figure 13 – System Open Loop Frequency Response

responsible for eliminating any steady state error. Figure 14 shows the new root locus for the compensated plant using this PI controller. Using this PI controller, the active magnetic thrust bearing was effectively stabilized. Appendix 8 shows the closed loop system using the plant transfer function and the PI controller. Here, the system was simulated for stability using this new controller. The purpose of modeling the system in such intricate detail should now be apparent. Through extensive modeling, it was possible to test any controller for the system and observe how the resulting system would respond. Steady state error, as well as stability could be analyzed before hard-coding anything. Therefore, modeling made it easy to predict how the system would respond and also provided an easy way to analyze any type of system failure.

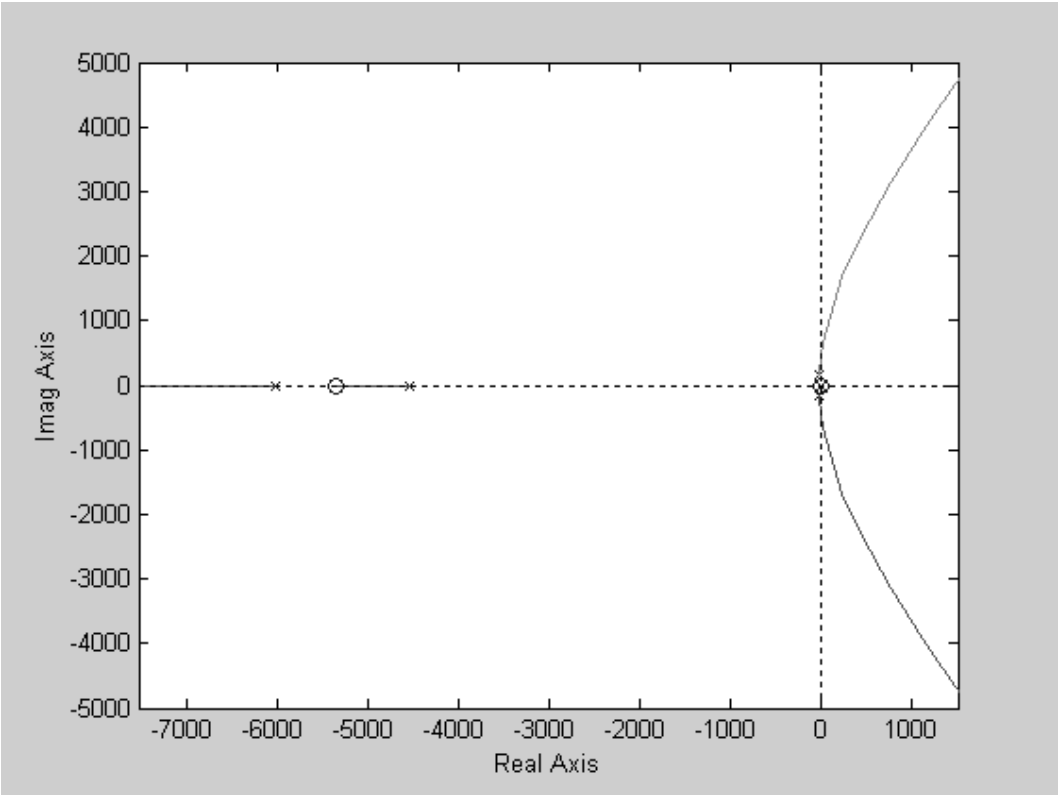

x = pole
o = zero

Figure 14 - PI Compensated System Root Locus

SYSTEMS DESIGN - ACTIVE SOUND CONTROL

AIR DUCT

The fan was placed about two inches inside a circular PVC pipe, whose inner diameter was 10 inches and whose length was 9 feet. The diameter was determined based on the existing fan blade, whose diameter was 8.875 inches. Thus, the fan's impeller took up almost all the diameter. The length was calculated based on the fan speeds, so as to obtain a standing wave within the pipe.

The slowest speed of the motor was around 430 rpm, while the motor was rated up to 10,000 rpm. The fundamental frequency of sound created from the fan blades was proportional to the speed of the motor. As they rotated and pushed air down the duct, the fan blade created a frequency of sound that was equal to the rotational rate in radians per second divided by 2π since 2π*f (Hz) = w (Rad/s). In addition to this frequency, there were additional tones related to the number of blades on the fan. Therefore, knowing the motor speed, it was possible to determine the tonal sound frequencies as well as the corresponding wavelengths. The latter property proved to be the most important in designing the pipe length, since the pipe must be long enough to support a standing wave. That is, the length of the pipe should ideally be a multiple of half a wavelength of a given frequency. A half-wavelength at 1000 rpm was 10.29 meters while a half-wavelength at 10,000 rpm was 1.029 meters. Operating at either extreme speed would allow for no adjustment in one direction.

The preliminary research called for an operating speed of 7500 rpm since it provided plenty of room for variation. In addition, the fundamental frequency associated with this speed is 125 Hz, corresponding to a wavelength of 2.744 meters, which is almost exactly 9 feet. However, further research proved that with the load of the fan, the motor could turn no higher than 6000

rpm. Also, it was found that when the fan was spun too fast, the duct would amplify its own resonant frequencies to the point that the fundamental noise of the fan would be unobservable on a sound spectrum plot. Therefore, a more realistic operating speed of 1800 rpm was chosen, which had a characteristic frequency of 30 Hz and therefore a characteristic wavelength of about 37.5 feet.[3] Therefore, a 9-foot long pipe is sufficient to support almost a standing quarter-wave.

In order for the pipe to support a standing wave in only the axial, and not radial direction, the diameter of the pipe had to be less than one-half the wavelength. Since the chosen diameter was only 10 inches, this criterion was satisfied, allowing sound waves to propagate only in the axial direction.

Background Work

As a precursor for the work that was done on active sound control, the sound signature of the rotating fan blade was observed using a digital signal analyzer: Siglab. Physically, Siglab is a small piece of equipment that transmits signals from a microphone to an interface on the computer, found within MATLAB. Siglab's virtual signal analyzer is very important for sound control since it shows the amplitude in decibels of sound produced at a range of frequencies. By taking sound measurements before and after the sound control algorithm was turned on, it was possible to observe whether or not sound was reduced at a particular frequency.

Five experiments were run in which the fan was spun at a different speed. For each trial, a microphone was placed in the duct so that it was less than a foot from the fan and an average signal over 100 seconds was recorded using the virtual signal analyzer. In all five cases, a small peak occurred at 60 Hz due to the 60 Hz electrical signal through the motor. However, a bigger

[3] The speed of sound is assumed to be 343 m/s

peak occurred at twice this frequency, or 120 Hz. In each case, a distinct peak was observed at the fundamental frequency due to the rotational rate. For example, when the fan was spun at 3000 rpm, a noticeable peak was seen at 50 Hz.[4] Again, at 3600 rpm, a noticeable peak was observed at 60 Hz, and so on. In addition, the biggest peak in each experiment was observed at three times the fundamental frequency since the fan has three blades. The reason is that the fan "chops" the air three times for every one revolution of the fan shaft. Harmonics of this frequency were also seen at twice, three times and even four times the blade rate.

Before active sound control could be achieved, it was important to study the sound dynamics of the pipe. Feeding a sine wave into the lead controller allowed the thrust bearing to oscillate at any specified frequency. Therefore, in theory, the microphone could observe this frequency over and above the fan noise.

During these investigations, it was found that some frequencies appear on the sound spectrum analyzer with little or no relevance to the thrust bearing's frequency of oscillation. Therefore, it was initially assumed that the duct was responsible for exciting these frequencies. To verify this claim, a few experiments were conducted. One included spinning the fan at a variety of different speeds, (3000, 3600, 4200, 4800, and 5400 rpm) while placing the microphone at the beginning of the pipe. The pipe's influence on sound was essentially eliminated in this experiment. No matter what the fundamental frequency of sound was due to the fan speed, none of the duct's frequencies appeared on the sound spectrum analyzer unless they were a multiple of the spin rate.

Another very important experiment was to run the fan at other speeds unrelated to the duct's excited frequencies. The results demonstrated that no matter what the speed of the fan, those

[4] (3000 rpm) * (1 min/60 sec) * (2π rad/rev) * (1 Hz / 2π rad/sec) = 50 Hz

certain frequencies appeared yet again.

In conclusion, when the duct's sound dynamics were eliminated, the unrelated frequencies were not present and when the duct was included, these frequencies were present no matter what the fan speed. Therefore, it was concluded that the duct indeed was exciting certain frequencies of sound, despite their unrelated nature to the fundamental frequency of the fan speed or frequency of the sine wave driving the controller.

An equation was found that relates resonant frequencies to the speed of sound and the length of pipe:

$$f = nc / 2l$$

where,

n = whole number multiples
c = speed of sound (343 m/s)[5]
l = length of duct (9ft = 2.7432 m)

Using these values (in the correct units), the following table shows the expected excitation frequencies versus the observed values:

Expected Frequencies (Hz)	Observed Frequencies (Hz)
62	65
125	115
187	180
250	235
312	295
375	350
437	410

Therefore, the observed resonant frequencies approximately matched the expected ones according to the above equation. These frequencies were important to know because when the sound control algorithm was implemented, it was necessary to know what frequency to examine

in the “before” and “after” sound spectrum graph. In addition, running the fan at any one of these frequencies will cause the sound to be amplified more than the normal amount since the duct will excite it naturally. Therefore, to aid in active sound control, the fan was run at a speed other than one of the natural frequencies of the duct.

ACTIVE SOUND CONTROL ALGORITHM

The method for achieving active sound control was to use a digital Finite Impulse Response (FIR) filter, G(z). Because its impulse response is a finite amount after some fixed time, it is inherently stable, unlike other types of digital filters [9]. Implemented as a C-program (shown in Appendix 14), it was used in this project to generate a signal, Y(z):

$$Y(z) = X(z)G(z) \qquad (14)$$

where X(z) is the input to the filter. In theory, Y(z) represented the z-transform of the original sound wave. Because sound waves typically resemble sine waves, the filter created a sine wave using 150 coefficients. This generated wave had the same amplitude, frequency, and phase of the original sound. The two sine waves were then *subtracted* from each other in order to achieve destructive interference.

A Least Mean Squares (LMS) algorithm adapted the coefficients of the FIR filter such that the square of the error between the original noise sound wave and the anti-noise sound wave was minimized according to the following equations [8]:

$$y(n) = \mathbf{w}^T(n)\mathbf{x}(n) \qquad (15)$$

$$e(n) = d(n) - y(n) = d(n) - \mathbf{w}^T(n)\mathbf{x}(n) \qquad (16)$$

where:

y(n) is the output of the filter

---

[5] The speed of sound varies with temperature. For average room temperature, it is assumed to be 343 m/s.

w(n) is a vector of adaptive coefficients

x(n) is the input

e(n) is the error between the desired signal, d(n) and output signal, y(n)

To produce a secondary sine wave, y(n), a reference sine wave, **x**(n), had to be generated that oscillated at the same frequency as the primary noise. To accomplish this, a sensor was installed on the motor that produced a voltage pulse for every one rotation of the impeller. By finding the period of this pulse train, it was possible to generate a sine wave of this frequency. This sine wave represented the fundamental frequency of the fan, due to the fan's rotational rate. Appendix 1 provides a more detailed discussion on the actual implementation of the period finder algorithm, while Appendices 10 and 11 show the block diagrams for the period finder and sine wave generator.[6]

The reference sine wave was the input to the FIR filter. The LMS algorithm used adaptive methods to change the filter coefficients, **w**(n), as it was running so that it constantly fine-tuned itself to cancel sound the best. In addition, having an adaptive filter let it adjust itself so that any desired frequency could be changed without having to rewrite the DSP program.

The output of the filter, y(n), was input to the thrust bearing's digital signal processor. More specifically, it went into the thrust bearing's controller, thereby forcing the impeller to oscillate at the fundamental frequency. The error signal, e(n), was provided by the error microphone, which will be discussed in further detail.

The only parameters of the LMS routine are the number of coefficients used to generate the secondary sine wave and the variable, μ, described below. Concerning the coefficients, the

[6] This algorithm was taken from "Active Noise Control," by Sen M. Kuo and Dennis R Morgan, 1996 [8]

algorithm becomes more accurate as the number of coefficients increases. However, too many coefficients can pose a problem if the digital sampling time is too small. In one sample time, the DSP must be able to process and calculate the values of all the coefficients. If the number of coefficients gets too big for the DSP to calculate within one sample time, there will be a lag in the creation of the sound controlling sine wave and it would not match the original sound wave very well. This project used 150 coefficients and the results demonstrated that it was a good choice.

The variable, μ, describes the step size of the routine as it refines the secondary sine wave in order to drive the error between the two waves to zero. As μ is increased, the error will converge to zero faster, but if it gets too big, the system will go unstable and sound control will not be achieved. Conversely, as μ is decreased, the time necessary for sound control will be longer but the system will remain stable. Thus, there is a trade-off between convergence time and stability.

Before implementing the DSP with the FIR filter downloaded to it, the sound control algorithm was simulated using MATLAB's Simulink. (See Appendix 12.) The simulation studied the effects of the number of coefficients and μ on sound attenuation.

The original design of the LMS routine called for it to be run from the d-SPACE real-time workshop. However, physical limitations of the computer would allow only around 10-15 coefficients of the filter to be downloaded to the DSP. Using this number of coefficients would inevitably lead to poor active sound control, since the actual number needed was at least 100. Therefore, it was evident that more electronic "horsepower" was needed. An external DSP was installed that received the reference sine wave from the dSPACE DSP and the microphone error signal as its two inputs. It then used a C-program that was downloaded to it for active sound control. However, the parameters from this program were controlled by the main (original)

computer. Like the rest of the system, these parameters could be changed in real time from the main computer. The output of this DSP went back into d-SPACE, where the sound controlling sine wave was fed into the thrust bearing's controller.

It was soon discovered that there was likely an impedance mismatch between the input and output of the external DSP. Therefore, the DSP was buffered from the actual input and output signals using voltage-following OP-AMPs. Furthermore, when the DSP outputted its defaulted signal (produced when the processor was reset) there appeared to be a DC offset voltage. To correct this, a high-pass filter was used consisting of an electrolytic capacitor and simple resistor.

In order to experiment with the sound control DSP, a simple C-program was written that would output a sine wave to an oscilloscope (See Appendix 13.) It was found that when the amplitude of the sine wave was below about 0.2, the signal would become lost in the noise. As the amplitude increased, however, the resolution increased, but above 1.1, the signal no longer resembled a sine wave at all. For the sake of good resolution, it was determined an amplitude at the upper end of this range was needed, and for simplicity, an amplitude of 1.0 was chosen. A sine wave of this magnitude could not be input into the controller since the total air gap in between the two sides of the thrust bearing was only 0.0014224 meters. Therefore a saturation block in Simulink was used to keep the signal within –0.0014 to +0.0014. It was soon determined that this fix would only cut off the signal and prevent the magnet's motion from resembling a true sine wave. Therefore, the output of the sound control DSP was first fed into a scaling gain, which scaled it down to the acceptable range. The signal was then input into the saturation block, which effectively acted as a secondary "safety net" to prevent the magnet from touching the sides of the bearing during sound control operations.

The error microphone was initially placed at the end of the pipe, but when sound control was initially attempted, it appeared that the algorithm was not working. Therefore, it was reasoned that the error microphone was too far from the fan and the fundamental frequency was lost in the pipe dynamics. The C-program previously mentioned for amplitude testing, was also used to generate a sine wave disturbance into the thrust-bearing controller. The sine wave would cause the rotor to oscillate back and forth, and would therefore cause the entire fan shaft to vibrate axially at a certain frequency and amplitude. Using real-time technology, it was possible to adjust the amplitude and frequency of this sine wave while the DSP was running. Since these vibrations caused noise, it would theoretically be possible to observe its frequency on a spectrum analyzer plot. Therefore, active sound control could only be achieved when the error microphone could distinguish the frequency of the sine wave output by the DSP.

The error microphone performed the critical function of measuring sound in the duct so that the DSP could measure the difference between the original sound and the output sound produced by the DSP controller. In theory, the controller would attempt to adjust its output signal until the error was driven to zero. In other words, it let the DSP know when the primary and secondary sound waves effectively canceled in destructive interference. It was found that at a distance of 3 feet from the fan, the error microphone could distinguish the frequency of any sine wave. With the error microphone at this position, sound control was now possible.

The performance microphone varied its position within the duct in order to measure the sound at multiple locations before and after the sound control algorithm was turned on in order to assure global sound control. Therefore, the error microphone could technically be placed at any position along the duct under two conditions. First, it must be able to distinctly hear any frequency of sound (up to the highest fan speed possible) over and above the pipe dynamics.

Second, the error microphone's position must remain constant during the experiment. That is, while the performance microphone's position

varied, the position of the error microphone had to remain fixed for consistency.

A sound spectrum graph in Figure 15a shows the sound at one point in the pipe with the fan running at 1800 rpm. Here, the sound control algorithm was not running.

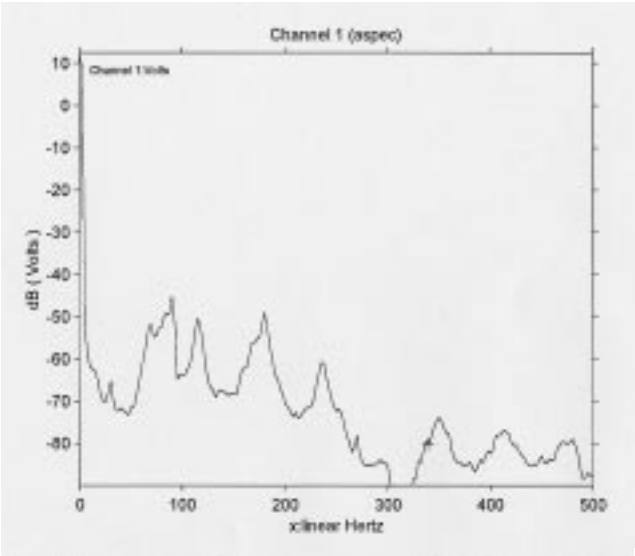

Figure 15a – Reference Plot, 30 Hz Fan

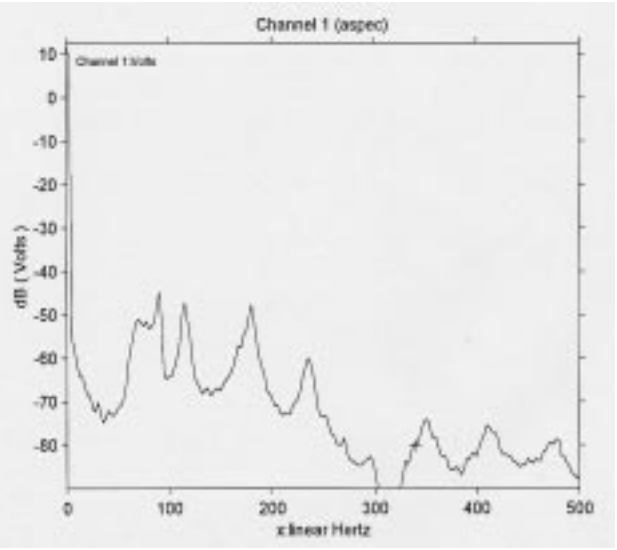

Figure 15b – Sound Control On, 30 Hz Fan

In addition to the 30 Hz peak, which is due to the fan speed, there exists a peak at 90 Hz, which is due to the fact that the fan has three blades on it. Also, there are the expected frequencies from the pipe dynamics. When the sound control was turned on, with the performance microphone at 7.5 feet from the fan, Figure 15b below demonstrates that the sound at 30 Hz is significantly lowered. The 30 Hz fan noise was attenuated at all points in the duct. Most points had, on average, 3.5 dB attenuation, although at a distance of 5.5 ft, there was only 1.3 dB attenuation. Interestingly enough, there was 6 dB of sound attenuation at a distance of 2 ft from the fan and 5 dB attenuation at 7.5 ft. The reason for these abnormalities in sound

attenuation has to do with the interference of the modes of the multiple standing waves in the duct. At some points, the modes naturally cancelled out the 30 Hz sound wave so that sound attenuation seems small. At other points, however, the modes added to the 30 Hz sound so that a much larger attenuation was observed. The following Microsoft Excel plot in Figure 16 shows the attenuation at discrete points in the duct, where the x-axis represents the distance in feet from the rotating fan.

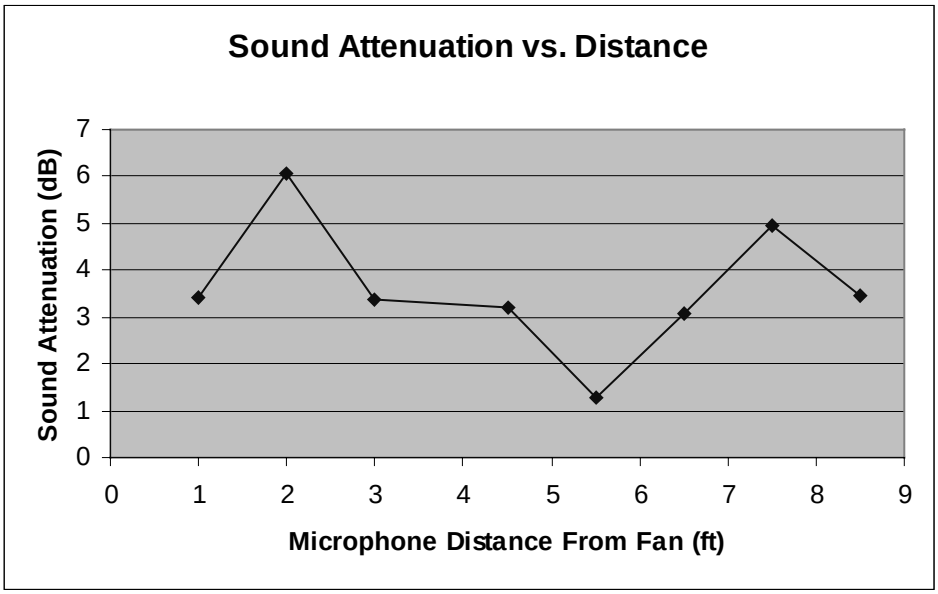

Figure 16 – Sound Attenuation Along the Duct

CONCLUSION

An active magnetic thrust bearing was stabilized using a PI compensator. It was then used to drive the fan's impeller at the same frequency and amplitude as the primary tonal noise from a rotating fan. The secondary noise, however, was driven out of phase with the primary noise in order to achieve destructive interference of sound.

Because the primary and secondary noise sources were collocated, global sound control of the fundamental frequency of rotation was successfully shown. Future work would include attenuating any single frequency due to the fan's rotational rate. Finally, broadband noise attenuation would be explored in which the sound control algorithm would lower the entire sound spectrum so that every frequency's associated sound level would be lower.

REFERENCES

[1] N.S. Nise, *Control Systems Engineering, Third Edition*. John Wiley & Sons, 2000

[2] L. O'Connor, "Active Magnetic Bearings Give Systems A Lift", Mechanical Engineering, July 1992, pp 52-57

[3] R.A. Serway, *Physics For Scientists & Engineers, Third Edition*. Harcourt Brace College, 1992

[4] J.M. Watkins, et al., *Adaptive Auto-Balancing Control of Magnetic Bearings For an Optical Chopper*, published in the Proceedings of the 2001 American Control Conference, June 2001, Arlington, VA

[5] J.M. Watkins, G.E. Piper, et al., *Global Control of Fan Noise In An Acoustic Duct Through The Use Of Magnetic Bearings*, published in the Proceedings of the 1999 American Control Conference, June 1999, San Diego, CA

[6] J.S. Wiggins, G.E. Piper, *Active Noise Control In Rotating Machinery Using Magnetic Bearings*, Proceedings of the IASTED International Conference, May 13-15, 1998, Pittsburgh, Pennsylvania, USA

[7] G. Schweitzer, H. Blueler, A. Traxler, *Active Magnetic Bearings, Basics, Properties and Applications of Active Magnetic Bearings*, Zurich, 1994

[8] S.M. Kuo, D.R. Morgan, *Active Noise Control Systems, Algorithms and DSP Implementations*, John Wiley & Sons, 1996

[9] P.A. Nelson, S.J. Elliott, *Active Control of Sound*, Harcourt Brace & Company, 1992

APPENDIX 1
JON'S HANDY HINTS

Pulse Train Period Finder

In order to generate a reference sine wave for the LMS algorithm, an additional algorithm had to be composed, which would read in the pulse train from a motor tachometer and generate a sine wave of the same frequency. This sine wave represented the fundamental frequency of sound created for any given fan rotational rate. The first part of the routine found the period of the pulse train, but it seemed rather noisy. Therefore, a first-order low-pass filter was used:

$$F(s) = a / (s + a)$$

It was found that a = 1 was a good value to filter out the noise. The benefit of using a small value was that the time constant was $\tau = 1/a = 1$ second. Therefore, the settling time was $4\tau = 4$ seconds and the noise could be filtered relatively quickly.

It was also found that when the fan is already spinning when the program is downloaded to a real-time interface, the system could track the period of the pulse train perfectly and generate a perfect sine wave. However, when the fan speed was adjusted during a real-time run, the period adjusted somewhat slowly to converge to its proper form despite the low settling time described above.

Therefore, the period finder algorithm works best if the fan is already spinning at a constant rate when the program is downloaded to the real time interface. Consequently, the algorithm cannot track a variable fan speed well. Therefore, if it is necessary to adjust the fan's speed, first adjust the speed, then rebuild the algorithm in the real-time interface.

In addition, the trigger, which was supposed to pick up each pulse, had trouble determining the separation between the actual pulses. Therefore, a relay block in Simulink was used in order

to cut off the top and bottom of the pulse signal, thereby making the pulse train cleaner and easier for the trigger to manage.

Active Sound Control

A real-time electronic switch was implemented so that at the click of the mouse, the sound control algorithm could be turned on or off. This control was needed in order to measure the sound with and without the sound control algorithm so that the program would not have to be rebuilt in between trials. However, it was discovered that the position of this switch in the block diagram was very important. Initially, it was positioned at the point in which the sound controlling sine wave entered the controller. However, this position did not prove advantageous. The reason is that after the program was built, the sound control switch was defaulted to the off position, but the error microphone continually reported that sound still existed in the pipe. Therefore, the sound control algorithm continued to increase the corrective sine wave, growing toward positive infinity over a short period of time. When the sound control switch was finally turned on, the amplitude was so big that the magnet crashed into the bearing immediately. In other words, the switch only prevented the sound controlling sine wave from reaching the controller without preventing it from building up so much.

A better solution was to place the switch physically *before* the sound control algorithm in order to prevent it from producing a sound control sine wave before the switch was turned on. This way, the sound control algorithm could begin producing its sound controlling sine wave only when the switch was turned on.

APPENDIX 2

```
%Midn 1/c Jonathan Nelson
%10/11/01
%Physical Parameter Script File for Thrust Bearings

x0=0.029 %nominal distance between magnet and each bearing, inches
Ai=1.244 %flux cross sectional area, inches^2
Ll1=611.67E-6 %leakage inductance, thrust bearing 1, H
Ll2=584.67E-6 %leakage inductance, thrust bearing 2, H
k01=0.002785  %k0 for thrust bearing 1, meters
k1=2.66E-7    %k for thrust bearing 1, meter-Henrys
k02=0.00347   %k0 for thrust bearing 2, meters
k2=2.119E-7   %k for thrust bearing 2, meter-Henrys
Rt1=3.13      %ohms
Rt2=3.83      %ohms
ksp=22000   %spring constant, N/m
m=0.640       %mass of thrust magnet, kg

%convert to metric units
x0=x0/39.3700787; %meters, (1 m = 39.3700787 in)
Ai=Ai/1550.0031;  %meters^2 (1 m^2 = 1550.0031 in^2)
```

APPENDIX 3

```
%Jon Nelson
%MATLAB m-file: Program to find the current through one of
%the thrust bearing magnets given the second current.
%Used to ensure that the force in each magnet is the same

i1=input('Enter i01: ');

k1=2.66e-7;  %m*H
k2=2.119e-7;  %m*H
k01=0.002785;  %m
k02=0.00347;  %m
x0=7.112e-4; %air gap, m

i2=(k02+x0)/(k01+x0)*sqrt(k1/k2)*i1;
disp('i2= ');
disp(i2);
```

APPENDIX 4

```
%Jon Nelson
%MATLAB m-file: Program to measure forces of thrust bearing
%given their currents magnets.
%Used to find nominal bias voltage

i1=input('Enter i01: ');
i2=input('Enter i02: ');

k1=2.66e-7;  %m*H
k2=2.119e-7;  %m*H
k01=0.002785;  %m
k02=0.00347;  %m
x0=7.112e-4; %air gap, m

fm1=k1/2*i1^2/(k01+x0)^2
fm2=k2/2*i2^2/(k02+x0)^2
```

APPENDIX 5

```
%Jon Nelson
%10/16/01
%The first part of this script file is to linearize a non-linear model
%of active magnetic thrust bearings
%The second part then converts this linear model into a linear transfer
%function
%and finds a corresponding lead controller
%This script file is based on the "jacobian" command and is based
%on a similar script file developed by Prof. Piper, 7/31/01
%NOTE: All units metric

%Define state variables
syms i1 i2
syms x1 x2
syms v

%Define inputs
syms e1 e2

%Define constants
syms k1 k2 k01 k02 x0 Ll1 Ll2
syms ksp m
syms e01 e02
syms Rt1 Rt2
syms i01 i02

x2=2*x0-x1;

%Inductances, etc.
L1=Ll1+k1/(k01+x1);     %total inductance of thrust bearing one
L2=Ll2+k2/(k02+x2);     %total inductance of thrust bearing two

%force equations
fm1=k1/2*i1^2/(k01+x1)^2;
fm2=k2/2*i2^2/(k02+x2)^2;
fs=ksp*(x1-x0);

%Electrical State Equations
di1=(e1-Rt1*i1+(k1*i1*v/(k01+x1)^2))/L1;
di2=(e2-Rt2*i2-(k2*i2*v/(k02+x2)^2))/L2;

%Mechanical State Equations
dx1=v;
dv=(-fm1+fm2-fs)/m;

%=========================================
%LINEARIZE MODEL
%=========================================
%state derivative vector
f=[di1; di2; dx1; dv];
```

```
%state vector
X=[i1; i2; x1; v];

%input vector
U=[e1; e2];

%output vector
%y=[x1];

%Jacobians
A=jacobian(f,X);
B=jacobian(f,U);
C=[0 0 1 0];

%==========================================
%Operating Conditions
i1=0.80;                   %current 1 at equilibrium
i2=1.07;                   %current 2 at equilibrium
e1=1;                   %equilibrium voltage across thrust bearing one
e2=1;                   %equilibrium voltage across thrust bearing two
x1=7.112e-004;             %nominal air gap
v=0;                       %at equilibrium, velocity=0

%Parameter values - constants (all units metric)
k1=2.66e-7;
k2=2.119e-7;
k01=0.002785;
k02=0.00347;
x0=7.112e-4;                  %nominal air gap (0.028 inches)
Ll1=6.1167e-004;              %leakage inductance of thrust bearing one
Ll2=5.8467e-004;              %leakage inductance of thrust bearing two
ksp=22000;                    %spring constant of motor/shaft coupling
ksensor=18/(2*x0);            %sensor gain=18V / total air gap
m=0.64;                       %mass of rotor
Rt1=3.13;                     %resistance of thrust bearing one
Rt2=3.83;                     %resistance of thrust bearing two
b=37.44;                      %damper value

%Substitute values into matrices
A=subs(A);
B=subs(B);
%C=subs(C);
B1 = B(:,1)-B(:,2);

%find plant transfer function, Gp(s) (linear approximation)
SS = ss(A,B1,C,[0]); %linear state equations for the plant
Gp = tf(SS);           %lienar transfer function for the plant
Gp=-1*Gp;               %take a minus sign out of plant for ease of %solving
                    %put a minus sign in controller later (-Kc)

%find design point
wn=200;     %natural frequency, (stiffness)
zeta=0.7;            %damping - found by trial and error to give correct
                     %design point and controller
theta=acos(zeta);    %design point angle, rad
```

```
thetadeg=theta*180/pi; %design point angle, deg
sigmad=wn*cos(theta);
omegad=wn*sin(theta);
sd=complex(-sigmad,omegad);  %design point

%find lead controller, part I
%define points in LHP are positive in value
%"      points in RHP are negative in value
kGc=evalfr(-1/Gp,sd);
mc=abs(kGc);            %magnitude of the controller
thetac=angle(kGc);      %angle of controller, rad
thetacdeg=thetac*180/pi;  %angle of controller, deg
alpha=pi-thetac;     %angle opposite thetac

%find PD zero
thetazpd=alpha;      %PD zero angle, rad
zpd=sigmad-(omegad/tan(thetazpd));
c=zpd;

%estimate lead zero
%d3=omegad/tan(pi-thetac);  %distance from design point to "c"
%c=sigmad-d3;              %point "c" of controller
zlead=c/2         %put zlead inbetween "c" and origin, in LHP
d1=sigmad-zlead;

%find lead controller, part II
thetaz=atan2(omegad,d1);
thetaz=pi-thetaz;
thetazdeg=thetaz*180/pi;
thetapdeg=thetazdeg-thetacdeg;
thetaprad=thetapdeg*pi/180;
d2=omegad/(tan(thetaprad));
p=sigmad+d2
mp=sqrt(d2^2+omegad^2);
mz=sqrt(d1^2+omegad^2);
kc=mc*mp/mz;
  kc=-1*kc                  %this -1 takes care of the -1*Gp above
```

APPENDIX 6
SPRING DAMPING

Actual Data - Set 1

Time	Volts
0.005	5.4
0.041	2.6
0.077	0.4

Exponential Best Fit Line

y = 7.8248e-36.148x

sigma_d = -36.148

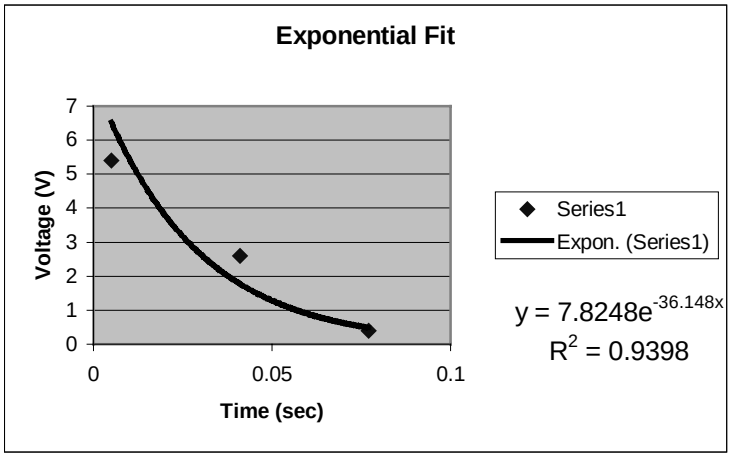

Actual Data - Set 2

Time	Volts
0.005	5.6
0.039	3.4
0.073	1

Exponential Best Fit Line

y = 7.1724e-25.335x

sigma_d = -25.335

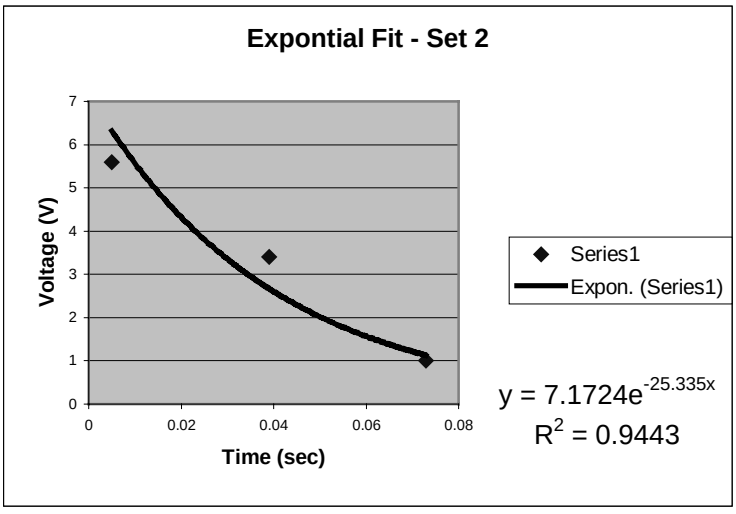

Actual Data - Set 3

Time	Volts
0.006	4.96
0.041	2
0.076	0.64

Exponential Best Fit Line
y = 6.1438e-29.253x
sigma_d = -29.253

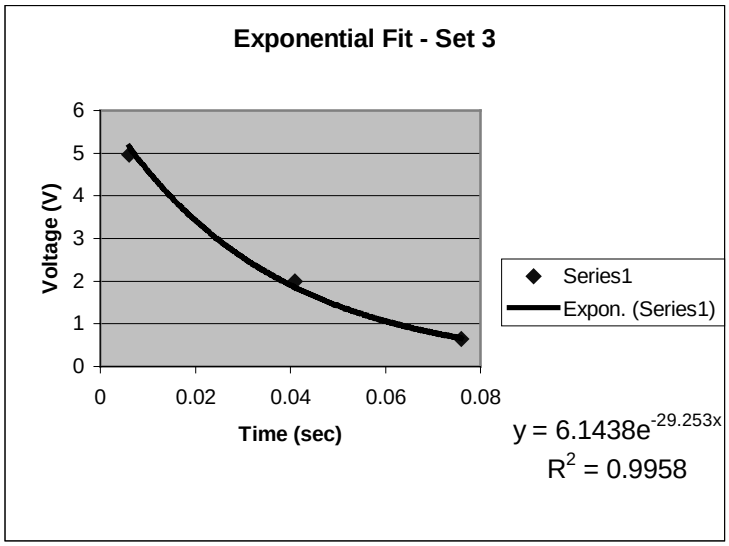

Actual Data - Set 4

Time	Volts
0.005	5.2
0.039	2.72
0.073	0.4

Exponential Best Fit Line
y = 7.7581e-37.72x
sigma_d = -37.72

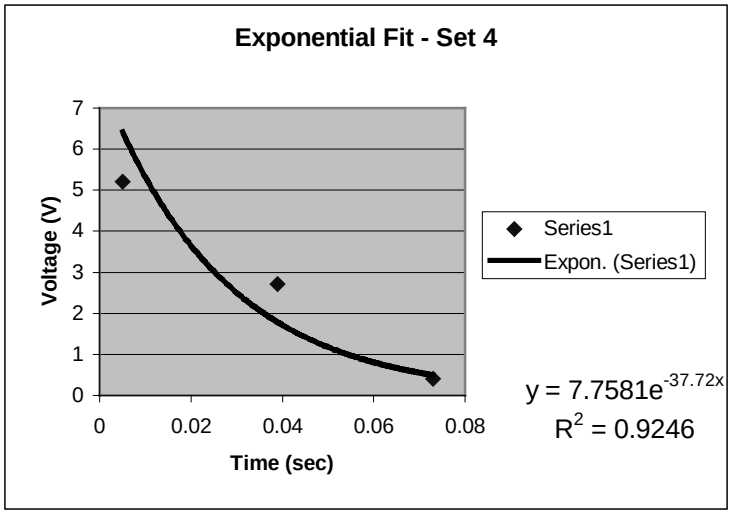

APPENDIX 7

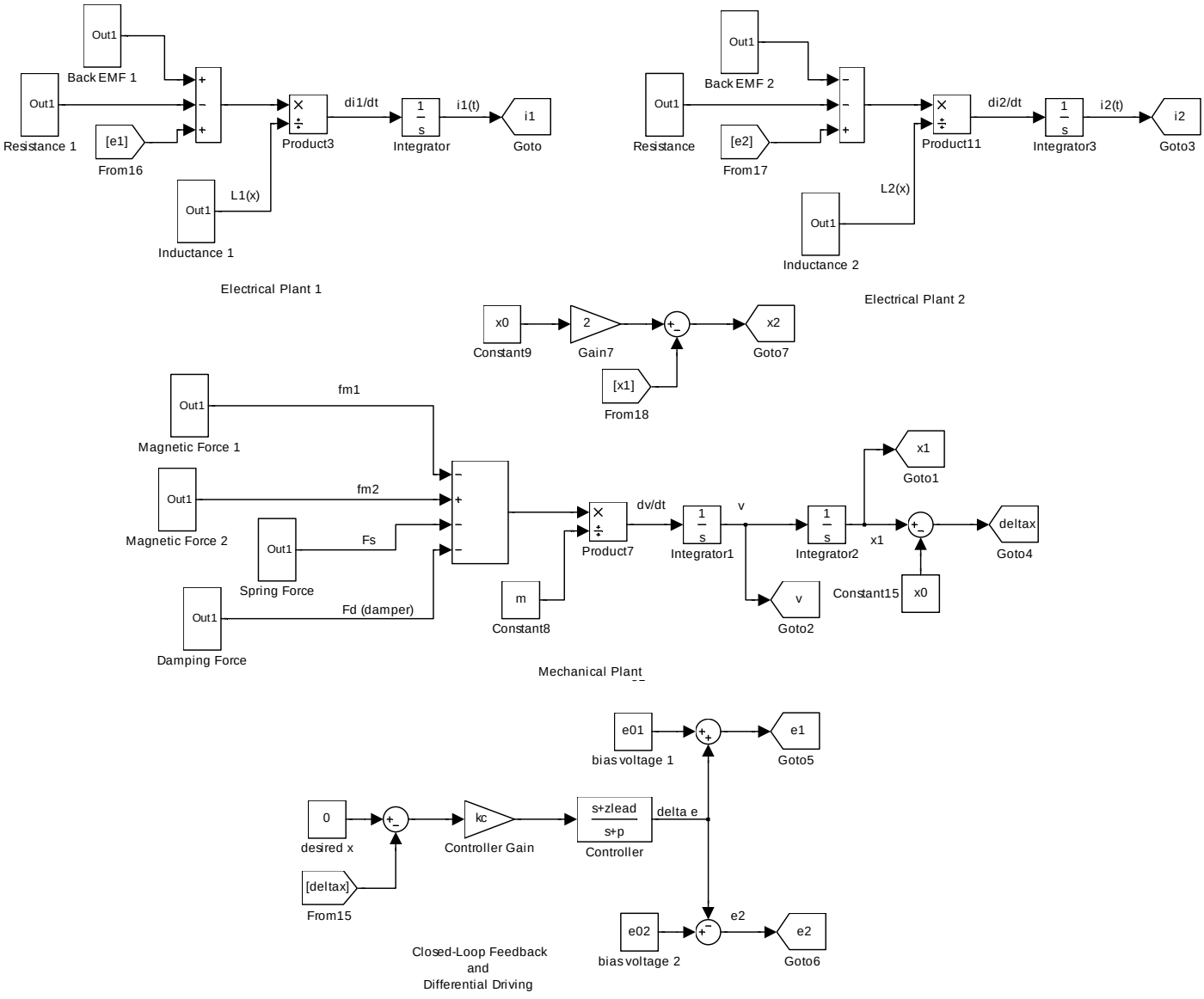
Out1
Back EMF 1
Out1
Resistance 1
[e1]
From16
Product3
di1/dt
Integrator
i1(t)
Goto
i1
Out1
L1(x)
Inductance 1
Electrical Plant 1
Out1
Back EMF 2
Out1
Resistance
[e2]
From17
Product11
di2/dt
Integrator3
i2(t)
Goto3
i2
L2(x)
Out1
Inductance 2
Electrical Plant 2
x0
Constant9
2
Gain7
x2
Goto7
[x1]
From18
Out1
Magnetic Force 1
fm1
Out1
Magnetic Force 2
fm2
Out1
Spring Force
Fs
Out1
Damping Force
Fd (damper)
m
Constant8
Product7
dv/dt
Integrator1
v
Integrator2
x1
Goto1
x1
deltax
Goto4
v
Goto2
Constant15
x0
Mechanical Plant
e01
bias voltage 1
e1
Goto5
0
desired x
kc
Controller Gain
s+zlead
s+p
Controller
delta e
[deltax]
From15
e02
bias voltage 2
e2
e2
Goto6
Closed-Loop Feedback
and
Differential Driving

APPENDIX 8

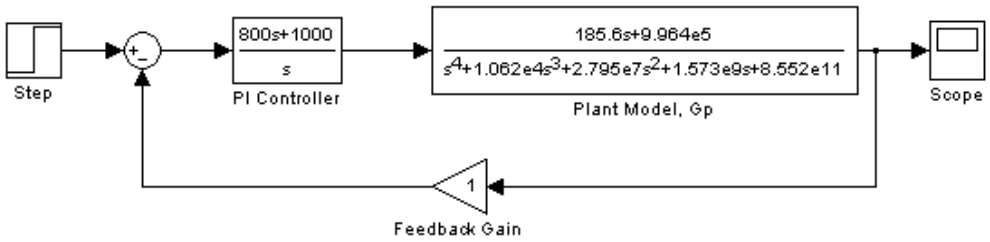

Closed Loop PI - Compensated System

APPENDIX 9

Thrust Bearing Controller and
Partial Sound Control Routine

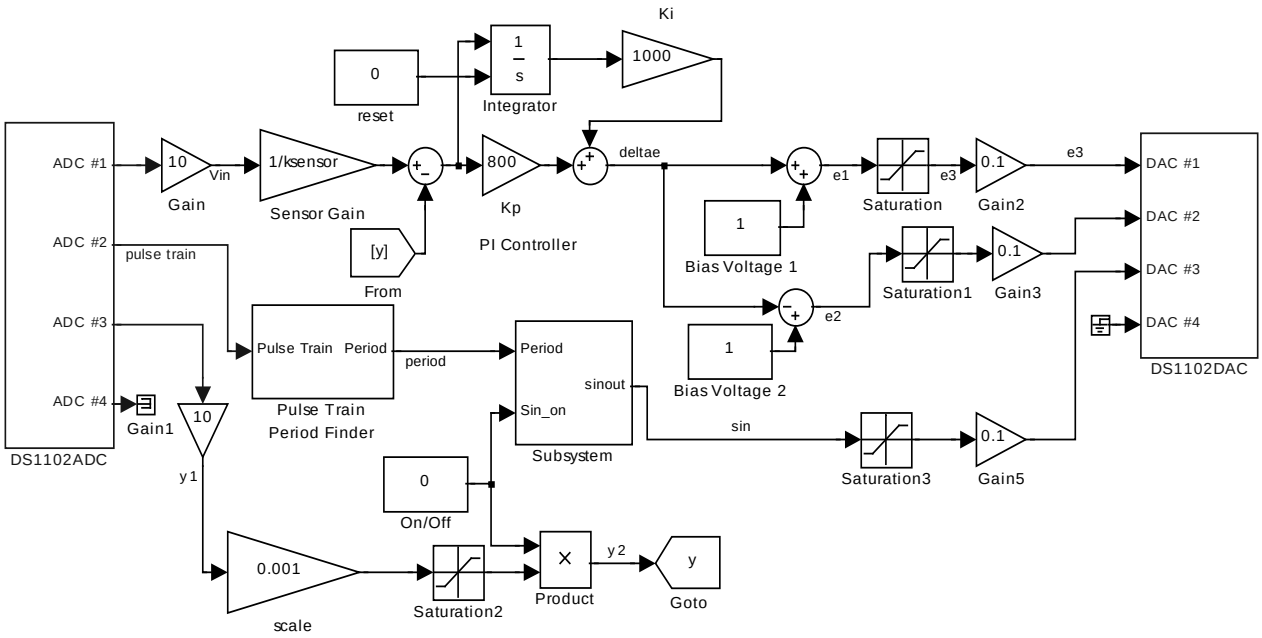

ADC1 from Scale and Shift Circuit
ADC2 from Motor Tachometer
ADC3 from output of Sound Control DSP

DAC1 to thrust bearing 1
DAC2 to thrust bearing 2
DAC3 to input1 of Sound Control DSP

APPENDIX 10

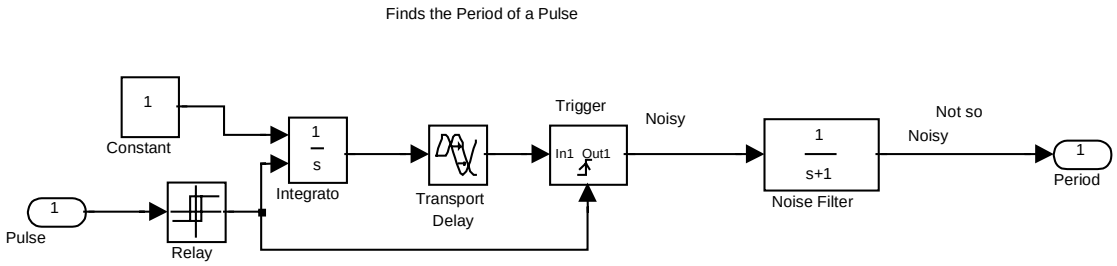

Pulse Train Period Finder

APPENDIX 11

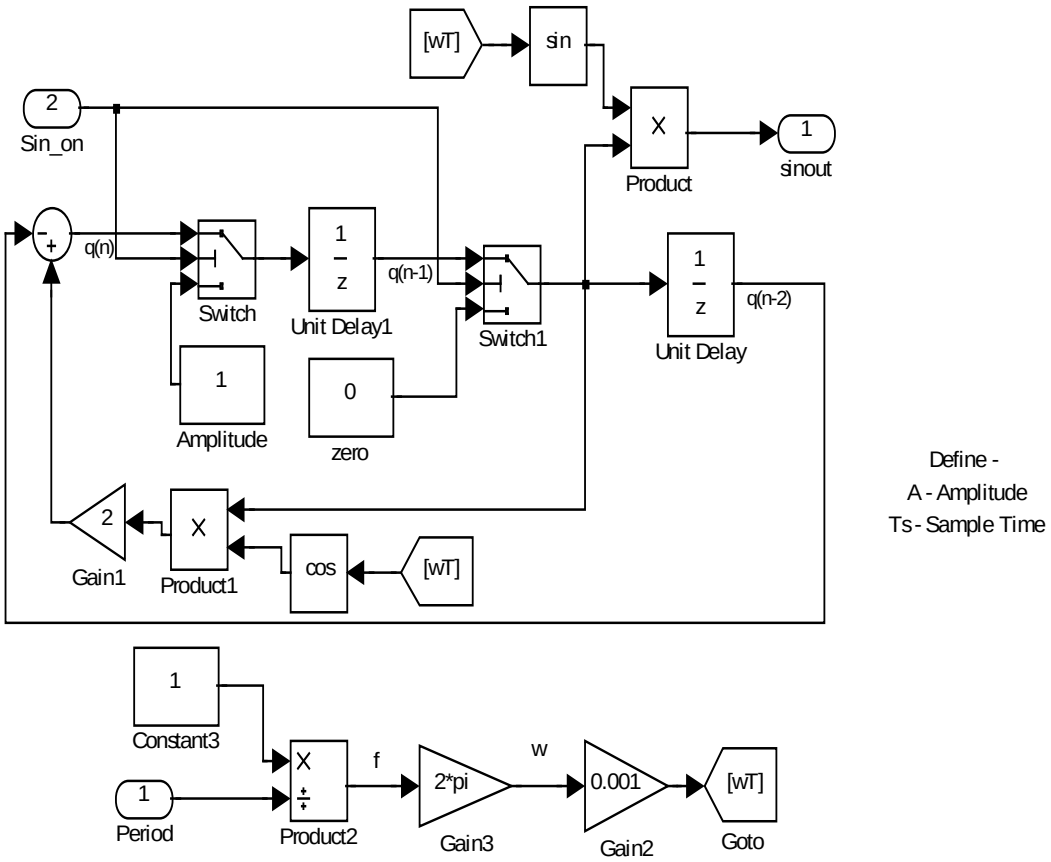

Reference Sine Wave Generator for Active Sound Control Algorithm

APPENDIX 12

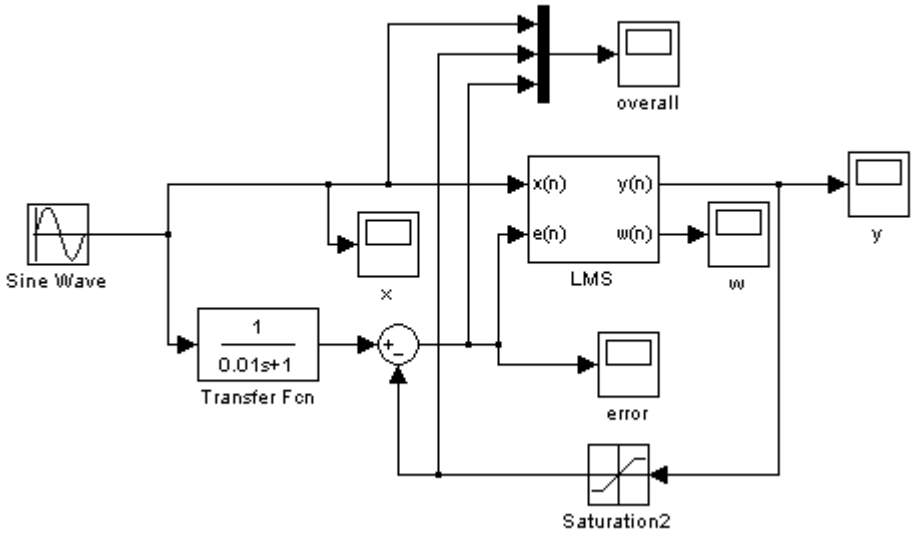

LMS Simulation

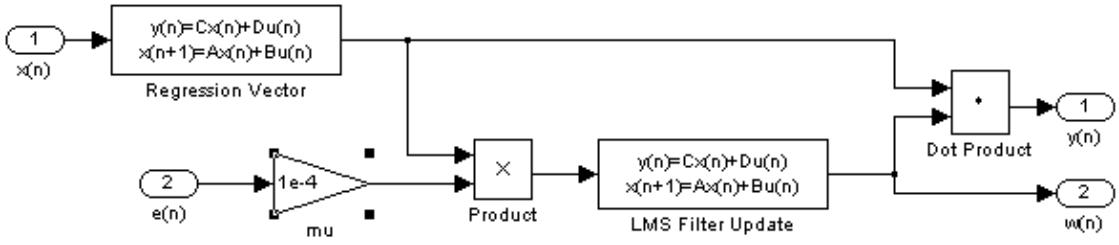

Sub-Block within LMS Simulation

APPENDIX 13

```
// ***********************************************************************
//                        SNDTST.C
//
                                                        **
//      Sine Wave Sound Test for EZ-KIT LITE
//      Written by:
//                    G. Piper  & J. Nelson  3/02
// ***********************************************************************

/* Input Gain formulae: CHAN1_GAIN * 1.5dB  (default CHAN1_GAIN = 0)
                        CHAN2_GAIN * 1.5dB  (default CHAN2_GAIN = 0)

Selecting CODEC samplerates:

SAMPLE_RATE  CODEC Rate (kHz)   SAMPLE_RATE   CODEC Rate (kHz)
         ( 0)         8              ( 1)         5.5125
         ( 2)         16             ( 2)         11.025
         ( 4)         27.42857       ( 5)         18.9
         ( 6)         32             ( 7)         12.05
         ( 8)         37.8           ( 9)         37.8
         (10)         44.1           (11)         44.1
         (12)         48 (default)   (13)         33.075
         (14)         9.6            (15)         6.615

*************************************************************/

#define SAMPLE_RATE 2     // Sets sample rate

#define CHAN1_GAIN 0      // Channel 1 gain factor
#define CHAN2_GAIN 0      // Channel 2 gain factor

#define N_TAPS 200        // Number of lms filter taps
#define IN_FACTOR 3.1/65536    // 3.1 volts per 16 bits
#define OUT_FACTOR 65536/2.2    // 16 bits per 2.2 volts

#include "ezsharc.h"   // Contains functions required for initialization
                       // plus the following user functions:

// ************  User function prototypes  ************
// float initialize( void );
// void get(int* _chan1, int* _chan2);
// inline extern int get_chan1( void );
// inline extern int get_chan2( void );
```

```
// void put(int chan1_, int chan2_);
// void put_chan1( int chan1_ );
// void put_chan2( int chan2_ );


// ************************  MAIN  *********************************

void main ( void )
{

  static int i = 0;
  static float amp = 1.0;
  static float f = 2;
  static float y;

  initialize();   // Initialize DSP

/* ---- Control Loop ----*/
  while(1)
  {
    idle();  // Wait for interrupt

    if( go ) // Check go flag
    {
      go = 0;   // Reset go flag

        y = amp*sin(f*i/57.3);
        i++;
        if( i > 360)
        {
                i =0;
        }

      put_chan1( (int)(OUT_FACTOR*y) );

    }

  }  /* end Control Loop */

}   /* end of main */
```

APPENDIX 14

```
// ***********************************************************************
//                        ANC.C
//
                                                        **
//      Active Noise Control program for EZ-KIT LITE
//      Written by:
//                    G. Piper  & C. Wick  3/98
// ***********************************************************************

/* Input Gain formulae: CHAN1_GAIN * 1.5dB  (default CHAN1_GAIN = 0)
                        CHAN2_GAIN * 1.5dB  (default CHAN2_GAIN = 0)

Selecting CODEC samplerates:

SAMPLE_RATE  CODEC Rate (kHz)   SAMPLE_RATE   CODEC Rate (kHz)
         ( 0)         8              ( 1)         5.5125
         ( 2)         16             ( 2)         11.025
         ( 4)         27.42857           ( 5)         18.9
         ( 6)         32             ( 7)         12.05
         ( 8)         37.8           ( 9)         37.8
         (10)         44.1           (11)         44.1
         (12)         48 (default)       (13)         33.075
         (14)         9.6            (15)         6.615

*************************************************************/

#define SAMPLE_RATE 2     // Sets sample rate

#define CHAN1_GAIN 0       // Channel 1 gain factor
#define CHAN2_GAIN 0       // Channel 2 gain factor

#define N_TAPS 150        // Number of lms filter taps
#define IN_FACTOR 3.1/65536    // 3.1 volts per 16 bits
#define OUT_FACTOR 65536/2.2    // 16 bits per 2.2 volts

#include "ezsharc.h"   // Contains functions required for initialization
                       // plus the following user functions:

// ************  User function prototypes  ************
// float initialize( void );
// void get(int* _chan1, int* _chan2);
// inline extern int get_chan1( void );
// inline extern int get_chan2( void );
```

```
// void put(int chan1_, int chan2_);
// void put_chan1( int chan1_ );
// void put_chan2( int chan2_ );


// ************************  MAIN  *********************************

void main ( void )
{

  static int i;
  static float x[N_TAPS];
  static float a_coeff[N_TAPS];
  static float y;
  static float error;
  static float mu = 0.000001;
  static int xout, yout;

  initialize();   // Initialize DSP

/* ---- Control Loop ----*/
  while(1)
  {
    idle();  // Wait for interrupt

    if( go ) // Check go flag
    {
      go = 0;   // Reset go flag

      /* Get reference signal */
      x[0] = (float)get_chan1()*IN_FACTOR;

         /* FIR Filter */
      y = 0.0;
         for( i=0; i<N_TAPS; i++ )
      {
        y = y + (a_coeff[i]*x[i]);
      }

      put_chan1( (int)(OUT_FACTOR*y) );

      /* Error signal */
      error = (float)get_chan2()*IN_FACTOR;

      /* Adaptive equation */
      for( i=0; i<N_TAPS; i++ )
```

```
        {
          a_coeff[i] = a_coeff[i] + (mu*x[i]*error);
        }

        /* Stage filter states */
        for( i=(N_TAPS-1); i>0; i--)
        {
          x[i] = x[i-1];
        }

      }

    }  /* end Control Loop */

}   /* end of main */
```